

Rothamsted Repository Download

A - Papers appearing in refereed journals

Lee, W-S., Devonshire, B. J., Hammond-Kosack, K. E., Rudd, J. J. and Kanyuka, K. 2015. Deregulation of plant cell death through disruption of chloroplast functionality affects asexual sporulation of *Zymoseptoria tritici* on wheat. *Molecular Plant-Microbe Interactions*. 28, pp. 590-604.

The publisher's version can be accessed at:

- <https://dx.doi.org/10.1094/MPMI-10-14-0346-R>

The output can be accessed at: <https://repository.rothamsted.ac.uk/item/8v050>.

© Please contact library@rothamsted.ac.uk for copyright queries.

Deregulation of Plant Cell Death Through Disruption of Chloroplast Functionality Affects Asexual Sporulation of *Zymoseptoria tritici* on Wheat

Wing-Sham Lee,¹ B. Jean Devonshire,² Kim E. Hammond-Kosack,¹ Jason J. Rudd,¹ and Kostya Kanyuka¹

¹Wheat Pathogenomics Team, Plant Biology and Crop Science Department, Rothamsted Research, Harpenden, AL5 2JQ, U.K.; ²Bioimaging, Plant Biology and Crop Science Department, Rothamsted Research, Harpenden, AL5 2JQ, U.K.

Submitted 29 October 2014. Accepted 1 December 2014.

Chloroplasts have a critical role in plant defense as sites for the biosynthesis of the signaling compounds salicylic acid (SA), jasmonic acid (JA), and nitric oxide (NO) and as major sites of reactive oxygen species production. Chloroplasts, therefore, regarded as important players in the induction and regulation of programmed cell death (PCD) in response to abiotic stresses and pathogen attack. The predominantly foliar pathogen of wheat *Zymoseptoria tritici* is proposed to exploit the plant PCD, which is associated with the transition in the fungus to the necrotrophic phase of infection. In this study virus-induced gene silencing was used to silence two key genes in carotenoid and chlorophyll biosynthesis, *phytoene desaturase (PDS)* and *Mg-chelatase H subunit (ChlH)*. The chlorophyll-deficient, *PDS*- and *ChlH*-silenced leaves of susceptible plants underwent more rapid pathogen-induced PCD but were significantly less able to support the subsequent asexual sporulation of *Z. tritici*. Conversely, major gene (*Stb6*)-mediated resistance to *Z. tritici* was partially compromised in *PDS*- and *ChlH*-silenced leaves. Chlorophyll-deficient wheat ears also displayed increased *Z. tritici* disease lesion formation accompanied by increased asexual sporulation. These data highlight the importance of chloroplast functionality and its interaction with regulated plant cell death in mediating different genotype and tissue-specific interactions between *Z. tritici* and wheat.

The ascomycete fungal pathogen *Zymoseptoria tritici* (synonyms: *Septoria tritici* and *Mycosphaerella graminicola*) is the causal agent of septoria tritici blotch (STB), one of the most economically important diseases of wheat in the United Kingdom and Western Europe (Dean et al. 2012). During infection of fully susceptible wheat genotypes, *Z. tritici* penetrates leaves exclusively via natural openings, i.e., the stomata. This is then followed by an extended period of symptomless infection that can last between 7 to 28 days, during which the fungus colonizes substomatal cavities and the apoplastic space around the mesophyll cells (Kema et al. 1996). Fungal biomass does not increase significantly until the next so-called necrotrophic phase associated with the rapid induction of host

cell death, release of nutrients and the appearance of disease lesions (Keon et al. 2007). Toward the end of this phase, asexual reproductive structures (pycnidia, which generate pycnidiospores) develop in the substomatal cavities and the fungus emerges from these in the form of cirri, containing mature pycnidiospores that can be propagated by rain-splash to other leaves, either on the same plant or on neighboring plants (Dean et al. 2012; Kema et al. 1996).

To date, eighteen resistance gene loci providing isolate-specific resistance to *Z. tritici* have been genetically mapped (Goodwin 2012), but none have yet been isolated. One of the most prevalent major resistance genes in elite wheat germplasm is *Stb6* (Chartrain et al. 2005). This gene is effective against the *Z. tritici* isolate IPO323 (Brading et al. 2002), for which the full genome sequence and genome annotation is available (Goodwin et al. 2011). One or more resistance mechanisms controlled by *Stb6* remain poorly understood. However, based on a variety of biochemical assays, it has been speculated that *Stb6* may be functioning to prevent wheat leaf cell death that normally occurs during a susceptible interaction, thus reducing or eliminating the formation of fungal pycnidia (Rudd et al. 2008).

The transition from the symptomless ‘biotrophic’ to the ‘necrotrophic’ phase of infection during the compatible interaction has been shown to involve a rapid and strictly localized form of programmed cell death (PCD), which has many similarities to the hypersensitive reaction (HR) in response to avirulent biotrophic pathogens directed by the plant disease resistance (*R*) genes (Keon et al. 2007; Rudd et al. 2008). This PCD response is associated with increased superoxide (O_2^-) and hydrogen peroxide (H_2O_2) accumulation and with degradation of host DNA from infected leaf cells into nucleosomal units (Keon et al. 2007). A precise mechanism of activation of PCD during *Z. tritici* infection remains to be determined, although it is likely to involve multiple signaling pathways.

It appears that several necrotrophic pathogens also manipulate host PCD to promote this response at one or more of the early phases of disease and thereby exploit these defense pathways to gain rapid access to nutrients for their own good (Mengiste 2012; Oliver and Solomon 2010). To facilitate plant cell death and stimulate susceptibility, necrotrophs generally secrete diverse phytotoxic metabolites, reactive oxygen species (ROS) and compounds inducing ROS generation, proteinaceous toxins, and a number of other effector proteins (Horbach et al. 2011; Oliver and Solomon 2010). One class of necrotrophic effectors that has received much interest is the host-selective toxins (HSTs) that are essential for fungal

Corresponding author: Kostya Kanyuka;
E-mail: kostya.kanyuka@rothamsted.ac.uk; Telephone: +44-1582-763133.

*The e-Xtra logo stands for “electronic extra” and indicates that nine supplementary figures and twelve supplementary tables are published online.”

pathogenicity and virulence on their host species (Wolpert et al. 2002). Quite often, only those host genotypes that carry genes conditioning sensitivity to HSTs become infected. Genes mediating sensitivity to HSTs victorin from *Cochliobolus victoriae* in *Arabidopsis thaliana* and ToxA from *Pyrenophora tritici-repentis* and *Stagonospora nodorum* in wheat have been isolated and were shown to encode plant disease resistance-like proteins (Faris et al. 2010; Lorang et al. 2007). These examples highlight the importance of PCD during the plant–necrotrophic fungi interaction. Plant disease resistance genes, plant-derived ROS, and host PCD have also been shown to play important roles in resistance to some necrotrophic and hemibiotrophic fungi (Asselbergh et al. 2007; Coego et al. 2005; Jia et al. 2000; Staal et al. 2008; Williams et al. 2011).

While the mitochondrion is known to play a prominent role in plant PCD (Lam et al. 2001), another possible key player in the induction and execution of plant PCD, including during the compatible *Z. tritici*–wheat interaction, is the chloroplast. First, chloroplasts are a major site of ROS production. H₂O₂, singlet oxygen, and superoxide anion radicals are generated in the photosystem reaction centers as byproducts of oxygenic photosynthesis when components of photosystem I and photosystem II (including the chlorophyll and carotenoid pigments) are unable to dissipate excess excitation energy (Asada 1999; Triantaphyllides et al. 2008). One of the important functions of ROS is mediation of chloroplast-to-nucleus retrograde signaling. In particular, ROS produced by chloroplast damage following exposure to high light can activate expression of nuclear-encoded genes, which leads to elicitation of PCD (Galvez-Valdivieso and Mullineaux 2010). Importantly, chloroplast-mediated ROS signaling appears to be involved in the activation of HR against invading pathogens (Kangasjärvi et al. 2012). Many plant mutants exhibiting spontaneous necrotic or chlorotic lesions that resemble pathogen-inducible HR (i.e., so-called lesion mimic mutants) have been shown to have defects in nuclear genome-encoded chloroplast-targeted proteins (Lorrain et al. 2003). Second, chloroplasts have an important role in a number of defense signaling pathways and host various steps in the biosynthetic pathways of different key signaling molecules, including SA, JA, NO (Creelman and Mullet 1997; Ishiguro et al. 2001; Jasid et al. 2006; Strawn et al. 2007).

The nuclear-encoded key enzymes in the biosynthesis of the pigments comprising a large part of the photosynthetic apparatus, phytoene desaturase (PDS) and Mg-chelatase H subunit (ChlH), have been widely used as markers in virus-induced gene silencing (VIGS) experiments. PDS catalyzes the rate-limiting step in carotenoid biosynthesis (Qin et al. 2007; Wang et al. 2009). Silencing of the *PDS* gene results in reduced carotenoid pigmentation and, as a result, also in reduced chlorophyll levels due to photo-oxidative damage. Thus, *PDS*-silenced leaves and floral tissues become photobleached (Kumagai et al. 1995). The other gene commonly used as a marker in VIGS, *ChlH*, is required, together with *ChlI* and *ChlD*, for the chelation of Mg²⁺ into protoporphyrin IX to generate Mg-protoporphyrin IX—the first committed step in the chlorophyll biosynthesis pathway (Masuda 2008). Silencing of *ChlH*, therefore, results in reduced chlorophyll levels in the chloroplasts, and *ChlH*-silenced leaves and floral tissues emerge an orange-yellow rather than white color due to the presence of other pigments (Hiriart et al. 2002; Papenbrock et al. 2000).

Ultrastructural studies have previously identified physical alterations of chloroplasts in wheat mesophyll cells during *Z. tritici* leaf infections (Kema et al. 1996). In this study, the ability of *Z. tritici* to infect chlorophyll-deficient *PDS*- and *ChlH*-silenced wheat leaf and ear tissues was investigated. We demonstrate that *PDS*- and *ChlH*-silenced leaves of susceptible plants undergo more rapid pathogen-induced cell death but are

significantly less able to support the asexual sporulation of *Z. tritici*. Conversely, leaves of resistant wheat, which normally do not undergo cell death, displayed disease lesion formation that was accompanied by an increase in asexual sporulation in this interaction. Moreover, wheat ears, which are not normally regarded as a significant host tissue for infection, also developed a greater number of asexual fungal sporulation structures in *PDS*- and *ChlH*-silenced plants. Collectively, these data highlight the importance of chloroplast functionality for the correct temporal regulation of plant cell death responses in different genotype- and tissue-specific interactions between *Z. tritici* and wheat plants.

RESULTS

The ability of *Z. tritici* to complete its asexual infection cycle is compromised in chlorophyll-deficient leaves of susceptible wheat plants.

First, the ability of *Z. tritici* to infect and cause disease on leaves of the susceptible wheat cultivar Riband, in which *TaPDS* or *TaChlH* genes were silenced using *Barley stripe mosaic virus* (BSMV)-mediated VIGS (Lee et al. 2012), was investigated. Inoculation of green leaves of virus-free (i.e., buffer-inoculated) or BSMV:*asGFP* control virus-infected plants with *Z. tritici* isolate IPO323 led to development of typical STB disease symptoms and dense coverage (>40%) of leaves by fungal pycnidia by 21 days postinoculation (dpi) (Figs. 1 and 2A). By contrast, no or only a few pycnidia formed on the chlorophyll-deficient leaves of BSMV:*asPDS*-infected or BSMV:*asChlH*-infected plants (Figs. 1 and 2A; Supplementary Table S1), although some signs of disease, such as tissue browning and sparse pycnidia, were noted in the green areas of non-uniformly silenced leaves (Supplementary Fig. S1).

Asexual sporulation of *Z. tritici* in wheat fields is stimulated by the high humidity environment created via a dense crop canopy and intermittent rainfall (Palmer and Skinner 2002). Previous laboratory experiments using diploid wheat *Triticum monococcum* demonstrated that pycnidia development and the release of pycnidiospores can be induced under high relative humidity (RH) conditions (>90%) in accessions that supported some *Z. tritici* hyphal growth in intercellular spaces but no sporulation under standard glasshouse conditions (approximately 60% RH) (Jing et al. 2008). To test whether *Z. tritici* sporulation could be induced in the chlorophyll-deficient leaves, fungus-inoculated leaves were detached from plants and were incubated at high RH for 48 h. Under these conditions a significant number ($P < 0.05$, least significant difference [LSD]) of the chlorophyll-deficient leaves become covered at moderate (40 to 60%) to high (>60%) density with black pycnidia-like structures (Figs. 1 and 2B). Upon closer examination, most of these structures appeared to be immature nonsporulating pycnidia (Supplementary Fig. S2; data not shown). Indeed, there was a 10- to 20-fold reduction in the numbers of pycnidiospores washed from *PDS*- and *ChlH*-silenced leaves compared with the corresponding positive control leaves (Fig. 2C).

Trypan blue was used to stain chlorophyll-deficient leaves at 21 days post-fungal inoculation prior to high RH incubation, in order to determine whether immature or nonmelanized pycnidia were present on these leaves. Fungal hyphae, stained blue, were visible in the intercellular spaces in the mesophyll cell layers but not the epidermal cell layer in *PDS*- and *ChlH*-silenced leaf tissue (Fig. 3). However, although pycnidia were visibly stained blue in control BSMV:*asGFP*-infected leaves at the corresponding time point, no pycnidia were visible in the chlorophyll-deficient leaf sections (Fig. 3).

To explore chlorophyll abundance, unstained but cleared leaf sections not infected by *Z. tritici* were examined using light

microscopy. Numerous chloroplasts were visible in mesophyll cells of control leaves, while few or no chloroplasts were visible in mesophyll cells in either *PDS*- or *ChlH*-silenced leaf tissue (Supplementary Fig. S3). This suggests that the chloroplasts were undeveloped or under-developed in the chlorophyll-deficient leaf tissue.

Scanning electron microscopy (SEM) reveals more rapid tissue collapse and substantial *Z. tritici* hyphal proliferation in chlorophyll-deficient leaves.

To gain a better insight into why silencing of wheat *PDS* or *ChlH* compromises asexual sporulation of *Z. tritici*, the fungus-infected VIGS treated leaves and the corresponding control leaves were examined using cryo-SEM during the late asymptomatic (14 dpi) and necrotrophic (21 dpi) phases of STB disease development. In control, BSMV:*asGFP*-treated leaves, abundant fungal hyphae were observed in the apoplastic space surrounding intact mesophyll cells (Fig. 4) and in substomatal cavities (data not shown) at 14 dpi with *Z. tritici* IPO323. At 21 days post-fungal inoculation, host cell death was widespread, as was the eruption of fungal spore masses (cirri) from mature

pycnidia onto the adaxial leaf surface (Fig. 4; data not shown). By contrast, in both *PDS*- and *ChlH*-silenced leaves, cell death was already prevalent at 14 dpi, with abundant fungal hyphae visible around collapsed mesophyll cells (Fig. 4). Importantly, cell structure and integrity was retained in chlorophyll-deficient leaves of a corresponding age in the absence of *Z. tritici*. Therefore, chlorophyll-deficient leaves appear to respond more rapidly to *Z. tritici*, requiring less time to undergo tissue death and collapse.

Interestingly, in *PDS*-silenced leaves, only a few hyphae were visible in the collapsed leaf tissue at 21 days post-*Z. tritici* inoculation. Instead, many protrusions under the cuticle, most likely representing subcuticular hyphae, were detected (Fig. 4; Supplementary Fig. S4). Subcuticular hyphae were not observed in *ChlH*-silenced leaves at a similar time point post-fungal inoculation (Fig. 4; data not shown).

Rapid tissue collapse is due to the early onset of host PCD in chlorophyll-deficient leaves.

In order to assess whether the rapid cell death response in chlorophyll-deficient leaves was, indeed, due to the early onset

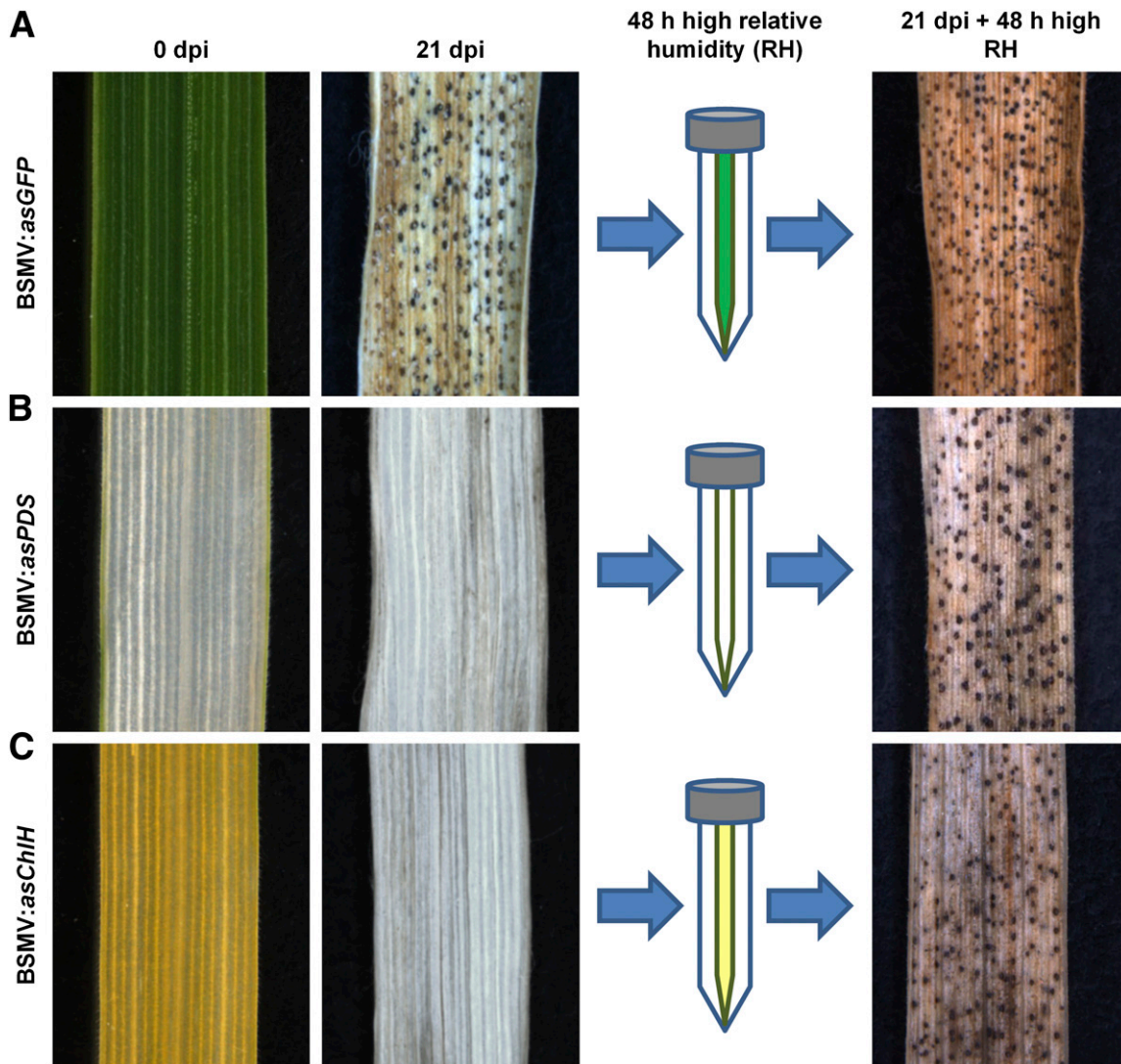


Fig. 1. Induction of visible leaf cell death and the formation of visibly melanized pycnidia by *Zymoseptoria tritici* on chlorophyll-deficient leaves require high relative humidity (RH) incubation. **A**, Lesions containing fungal pycnidia are visible at 21 days postinoculation (dpi) with *Z. tritici* on virus control-infected (BSMV:*asGFP*) leaves of wheat cv. Riband. **B**, No pycnidia are visible at 21 dpi on photobleached (chlorophyll deficient) *phytoene desaturase*-silenced (BSMV:*asPDS*) or **C**, *Mg-chelatase H subunit*-silenced (BSMV:*asChlH*) leaves unless the photobleached leaves are detached and placed at high RH conditions for a further 48 h (21 dpi + 48 h high RH).

of host PCD, we investigated the integrity of host genomic DNA in *PDS*-silenced leaf tissue over a time course of *Z. tritici* infection. This revealed laddering of DNA extracted from *PDS*-silenced leaves at 7 and 9 dpi with *Z. tritici* (Supplementary Fig. S5A), suggesting that PCD rather than uncontrolled cellular disintegration was triggered in these tissues. Changes in membrane integrity in control and *PDS*-silenced leaf segments over the same *Z. tritici* infection time course were also assayed by measuring electrolyte leakage into an ion-free bathing solution of deionized water. A strong increase in electrolyte leakage, as indicated by increased conductivity of the bathing solution, was observed in samples taken between 10 and 14 dpi from *PDS*-silenced leaf tissue. This increase was not observed in *PDS*-silenced leaves in the absence of *Z. tritici* infection.

A more gradual loss of membrane integrity was measured in control-treated leaves from 12 dpi onward.

H₂O₂ accumulates more rapidly during *Z. tritici* infection of chlorophyll-deficient leaves.

Previous studies have shown that the onset of visible disease symptoms coincides with the rapid increase in accumulation of O₂⁻ and H₂O₂ in *Z. tritici*-infected leaf tissue (Keon et al. 2007; Shetty et al. 2003), although it was not clear to what extent these ROS originate from the plant or the fungus. Control-treated and *PDS*- and *ChlH*-silenced leaves were collected throughout the *Z. tritici* infection time course and were stained with diaminobenzidine (DAB) to visualize H₂O₂ (Thordal-Christensen et al. 1997). Strong brown DAB staining was

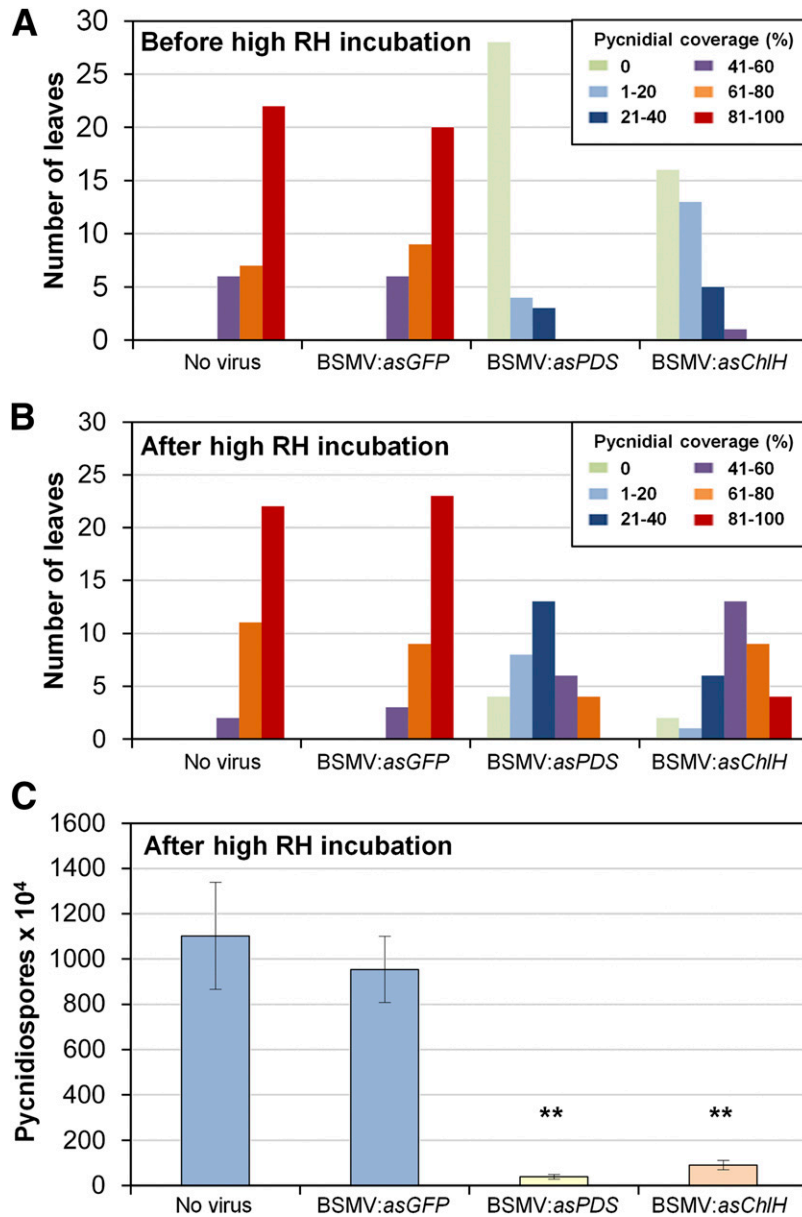


Fig. 2. The *Zymoseptoria tritici* pycnidia induced on chlorophyll-deficient leaves by high relative humidity (RH) incubation contain few pycnidiospores. Leaves of control-treated (no virus and BSMV:asGFP) and chlorophyll-deficient (BSMV:asPDS and BSMV:asChlH virus-induced gene silencing treated) wheat cv. Riband were inoculated with *Z. tritici*. The percent pycnidial coverage was scored at 21 days postinoculation (dpi) either **A**, before further incubation at high RH or **B**, after 48 h at high RH (21 dpi + 48 h high RH). Data plotted are the total number of leaves within each of the six pycnidial coverage score classes, where a total of 35 leaves per virus treatment were scored over four independent experiments. **C**, Mean pycnidiospore counts in spore washes from detached leaves after 48 h of incubation at high RH. Data shown are mean spore counts from a minimum of nine samples from three independent experiments. One sample comprised 3 × 6-cm-long leaf segments, each leaf from an individual plant. Error bars represent mean ± standard error of the mean. Double asterisks denote $P < 0.01$ from restricted maximum likelihood analysis.

observed only in control-treated leaves collected at 14 dpi and not in leaves sampled at earlier time points post-fungal inoculation (Fig. 5A). By contrast, levels of H₂O₂ were found to be elevated even at 9 dpi in *PDS*- and *ChlH*-silenced leaves, when compared with corresponding leaf sections collected at 0 dpi (Fig. 5A). Moreover, DAB staining revealed that H₂O₂ was already produced in *ChlH*-silenced leaves prior to inoculation with *Z. tritici* (Fig. 5A). However, H₂O₂ levels as indicated by the intensity of DAB staining, were similar in *PDS*- and *ChlH*-silenced leaves collected at 0 dpi and 14 dpi time points (corresponding to 14 and 28 days post-virus inoculation, respectively) in the absence of *Z. tritici* infection (Fig. 5A). This suggests that H₂O₂ accumulation in chlorophyll-deficient leaves is specifically induced in response to fungal infection. Closer inspection of DAB-stained *PDS*- and *ChlH*-silenced leaves at 14 dpi indicated that H₂O₂ accumulated in the mesophyll cells and not in the epidermal cell layers (Supplementary Fig. S6; data not shown). Hyphae of *Z. tritici* were found not to be stained by DAB, thereby indicating that the additional H₂O₂ detected was produced or released by the plant.

To independently verify that H₂O₂ accumulated in *ChlH*-silenced leaves in the absence of *Z. tritici* infection, a peroxidase-coupled colorimetric assay was used to measure basal H₂O₂ levels in control-treated and chlorophyll-deficient leaves that were not subjected to *Z. tritici* inoculation. As expected, significantly higher levels of total H₂O₂ ($P < 0.05$) were measured in *ChlH*-silenced but not in *PDS*-silenced or the control-treated

leaf samples (Fig. 5B). This trend was observed in two independent experiments and agreed well with the DAB staining results (Fig. 5A).

Collectively, these data suggest that ROS accumulated in the chlorophyll-deficient *PDS*- and *ChlH*-silenced leaves as a result of photo-oxidative damage, which correlated with a more rapid onset of the host PCD during *Z. tritici* infection.

***Stb6*-mediated resistance to *Z. tritici* is partially compromised in chlorophyll-deficient leaves.**

Given the involvement of the chloroplast in the biosynthetic pathways of multiple defense signaling compounds, ROS production, and induction of PCD, we tested whether this organelle might also play a role in incompatible wheat-*Z. tritici* interactions. The effect of silencing *PDS* and *ChlH* on the outcome of an incompatible wheat-*Z. tritici* interaction was investigated using the wheat cvs. Cadenza and Chinese Spring carrying the *Stb6* gene for resistance to the *Z. tritici* isolate IPO323.

No fungal pycnidia were visible at 21 dpi on either the chlorophyll-deficient or virus control-treated leaves of *Stb6* containing cultivars (Fig. 6A to C and F). However, when the leaves were incubated at high RH conditions for 48 h, pycnidia appeared on a significant number of *PDS*- and *ChlH*-silenced leaves of both cvs. Cadenza and Chinese Spring (when compared with virus control-treated leaves; $P < 0.05$, LSD), albeit at predominately low to moderate density (Fig. 6A to B, D, and G). There was no significant difference between the percent pycnidial coverage profiles of the two cultivars ($P = 0.714$,

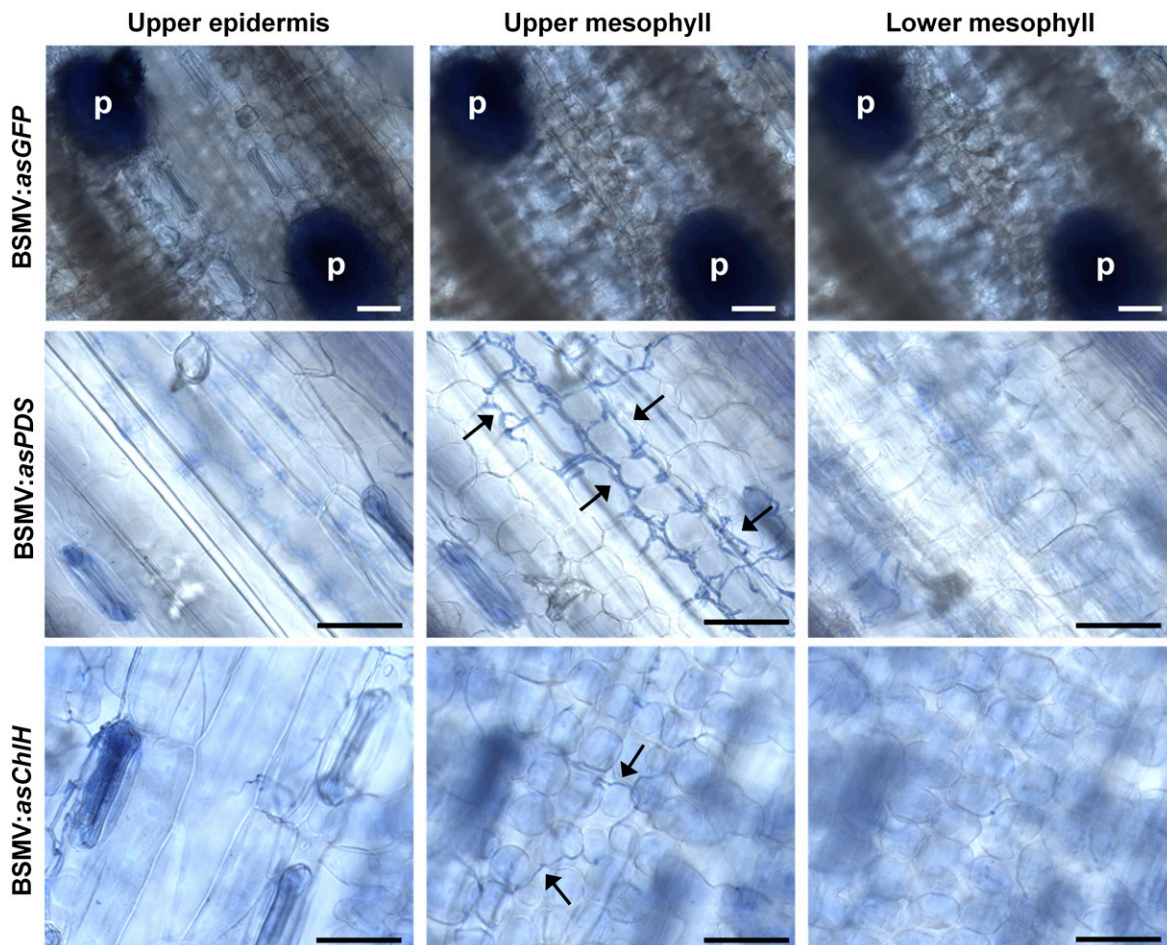


Fig. 3. Assessment of the extent of *Zymoseptoria tritici* hyphal colonization and development in the wheat leaf epidermal and mesophyll cell layers by trypan blue staining. Leaf segments from virus control (BSMV:asGFP) and chlorophyll-deficient (BSMV:asPDS and BSMV:asChlH) leaves at 21 days post-inoculation with *Z. tritici* were stained with trypan blue. Arrows indicate fungal hyphae; p, pycnidia. Scale bars represent 50 μ m.

F test; Supplementary Table S2). Relatively small numbers of pycnidiospores were obtained in washes from these leaves, indicating that the majority of pycnidial structures observed were immature (Fig. 6E and H). Nevertheless, significantly more spores were obtained from *PDS*-silenced ($P < 0.05$, LSD) and *ChlH*-silenced leaves ($P < 0.01$, LSD) than from virus control-treated leaves of cv. Chinese Spring (Fig. 6H). There was also a trend for higher numbers of pycnidiospores washed from chlorophyll-deficient vs. green cv. Cadenza leaves (Fig. 6E), although the difference was at a low level of statistical significance ($P > 0.05$). This experiment was carried out three times with both cvs. Cadenza and Chinese Spring, with consistent results.

Leaf tissues from cvs. Chinese Spring and Cadenza that had not been inoculated with *Z. tritici* were stained with DAB to determine whether chlorophyll-deficient leaves from these cultivars also accumulated higher basal levels of H_2O_2 . As was the case with susceptible cv. Riband, in resistant cv. Chinese Spring, stronger staining was observed in *ChlH*-silenced leaf tissue than in virus-control or in *PDS*-silenced leaves (Supplementary Fig. S7). By contrast, in cv. Cadenza, both the *PDS*- and *ChlH*-silenced leaves only showed weak DAB staining that was only slightly stronger than that observed with virus control-treated leaves. These data suggest that

different cultivars may respond differently to a lack of chloroplast function.

***PDS*- and *ChlH*-silenced wheat ear tissues are less resistant to *Z. tritici* infection.**

Z. tritici is considered to be almost exclusively a foliar pathogen and under standard field conditions wheat ears usually appear to be free of STB symptoms (Eyal 1999), although there are reports of successful fungal DNA detection in wheat chaff and seeds by sensitive polymerase chain reaction (PCR) methods and of pycnidia-like lesions on glumes in high STB disease pressure years (Consolo et al. 2009; B. Fraaije *personal communication*). However, these assays did not demonstrate that the fungal material detected was in the form of sporulating pycnidia resulting from a completed asexual cycle in ear tissue. Here, the possibility of inducing partial or full STB disease on ears of spring wheat cv. Bobwhite, fully susceptible to *Z. tritici*, using controlled spray inoculation with conidiospores was formally explored. We also investigated whether silencing of *PDS* and *ChlH* in wheat ears affected the outcome of these interactions.

Three different *Z. tritici* conidiospore concentrations (5×10^5 , 5×10^6 , and 1×10^7 spores per milliliter) were tested in initial spray-inoculations of attached wheat ears when the

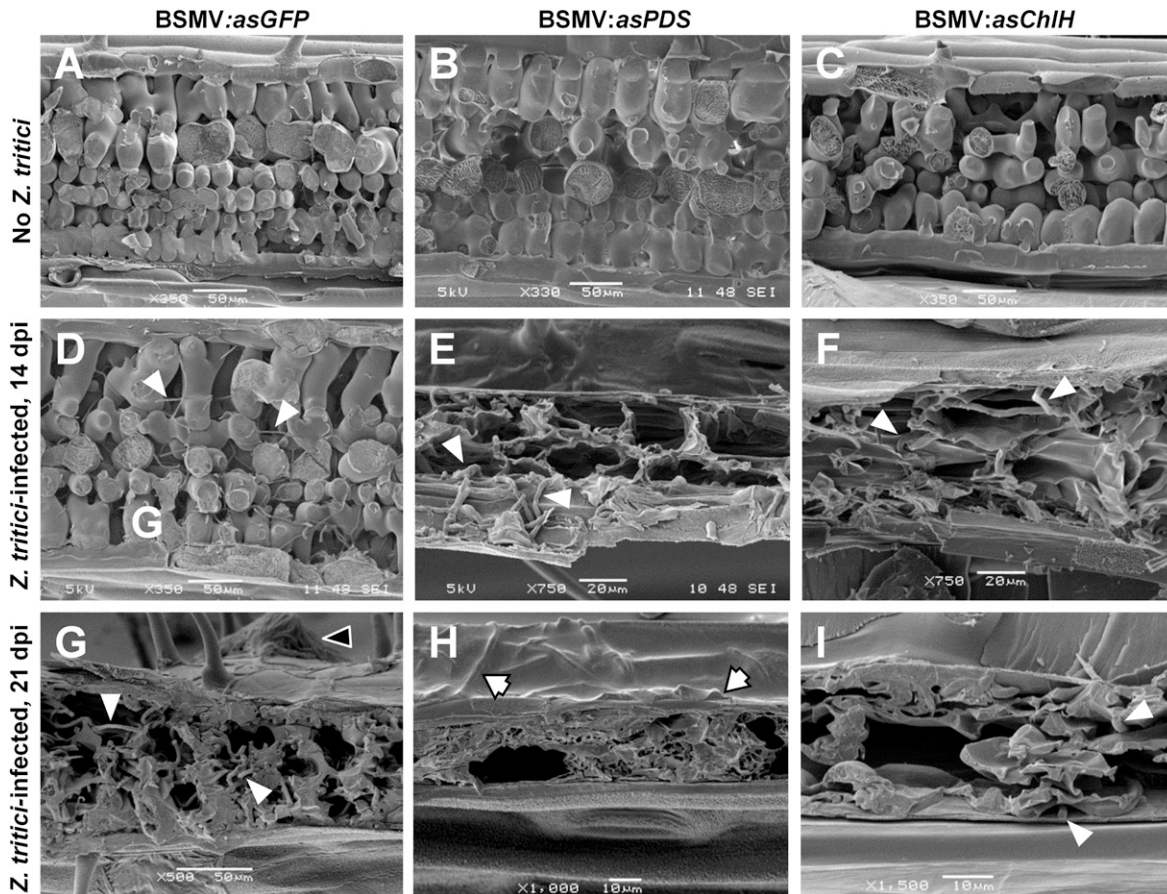


Fig. 4. Cryo scanning electron microscopy (cryo-SEM) of *Zymoseptoria tritici*-inoculated leaves reveals more rapid host cell death and tissue collapse in response to *Z. tritici* infection in chlorophyll-deficient leaf tissue. SEM images are of control-treated (BSMV:asGFP, left column), *phytoene desaturase* (*PDS*)-silenced (BSMV:asPDS, middle column) and *Mg-chelatase H subunit* (*ChlH*)-silenced (BSMV:asChlH, right column) leaves of wheat cv. Riband. **A to C**, The appearance of healthy epidermal and mesophyll cells in control-treated and chlorophyll-deficient leaf sections in the absence of *Z. tritici* inoculation. The leaf sections were from the fourth leaf of 39-day-old plants at 28 days postinoculation (dpi) with virus. **D to F**, Leaf sections at 14 dpi with *Z. tritici*. Fungal hyphae are visible around intact plant cells in virus control leaves (**D**), but thicker hyphae surround collapsed dead plant cells in *PDS*- (**E**) and *ChlH*-silenced (**F**) leaves. **G to I**, Leaf tissue sections at 21 dpi with *Z. tritici*. **G**, Abundant fungal hyphae surrounded by dead cells in virus control leaves. The white-edged black arrowhead indicates a mass of pycnidiospores visible on the outer leaf surface. **H**, Black-edged arrows indicate subcuticular hyphae under the leaf cuticle in *PDS*-silenced leaves. Abundant fungal hyphae surrounded by dead plant cells are visible. **I**, Abundant fungal hyphae in *ChlH*-silenced leaf tissue. In panels **D** through **G**, white arrowheads highlight representative *Z. tritici* hyphae visible in all tissues. White scale bars represent 10, 20, or 50 μ m as indicated.

plants were just commencing anthesis. Pycnidia developed on the tips of a measurable but small percentage of florets on inoculated ears following inoculation with 5×10^6 spores per milliliter (Supplementary Fig. S8). This spore concentration was used for subsequent experiments. Interestingly, pycnidia only appear to develop on the glume tips, which have regions of green (chlorophyll-containing) tissue, or on the awns and, occasionally, the very tip of the lemma adjacent to the awn (Fig. 7).

Virus control-treated and *PDS*- and *ChlH*-silenced ears of wheat cv. Bobwhite were spray-inoculated with conidiospores of *Z. tritici* IPO323 in three independent experiments. As expected, pycnidia only developed at a very low density on approximately 12% of the florets on BSMV:*asGFP* (virus control)-treated ears (Fig. 7B and D; data not shown). By contrast, a moderate to high density of pycnidia were visible on a significantly higher proportion of florets on both *PDS*-

silenced (65.8%) and *ChlH*-silenced ears (47.4%) ($P < 0.01$, LSD). Many of these pycnidia contained pycnidiospores emerging from stomata in cirri (data not shown), and significantly more spores were detected in water washes from the chlorophyll-deficient ears than in washes from control-treated ears (Fig. 7C to E) ($P < 0.01$, LSD). On average, between 5 and 5.5 million pycnidiospores were sampled from each of the chlorophyll-deficient ears, while only 2 million spores were washed from control-treated ears (Fig. 7E).

To verify that the *Z. tritici* spores washed from *PDS*- and *ChlH*-silenced wheat ears were viable, the retrieved spores were inoculated onto leaves of fully susceptible cv. Riband. By 21 dpi, all the inoculated leaves developed necrotic lesions and mature pycnidia characteristic of STB disease (Supplementary Fig. S9). These data confirmed that *Z. tritici* is able to complete an asexual reproductive cycle on green tissues of wheat ears

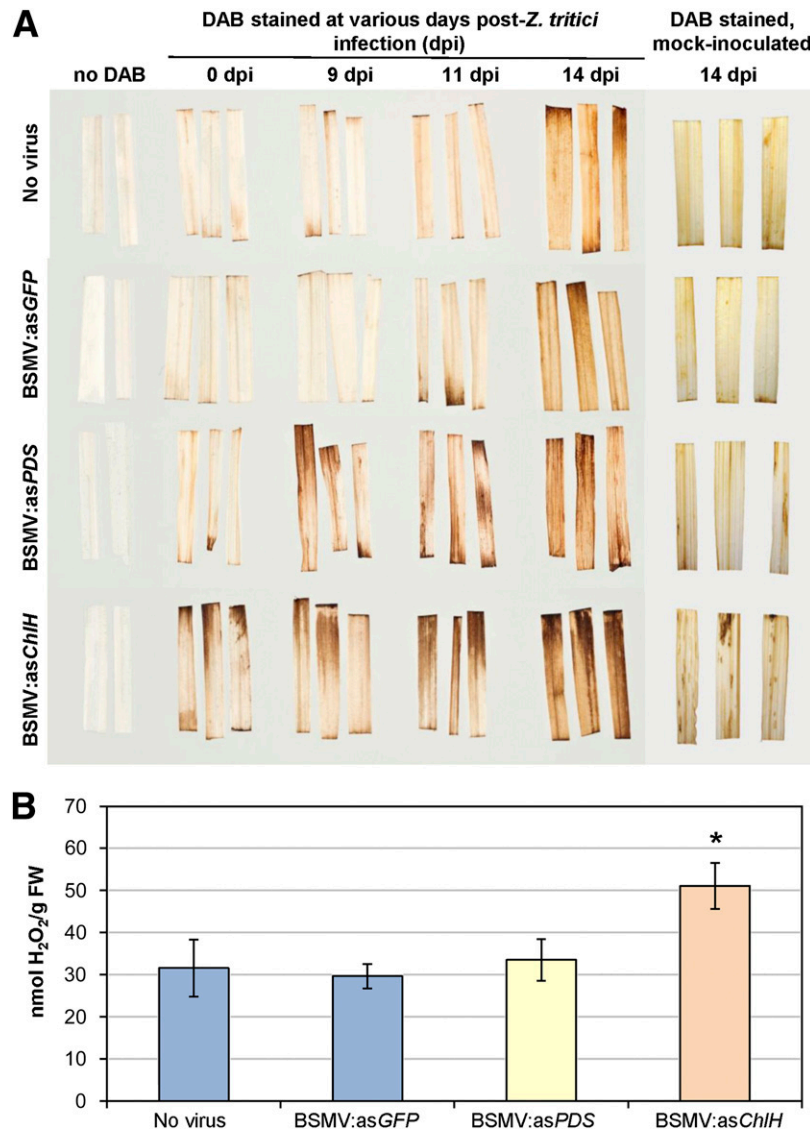


Fig. 5. Chlorophyll-deficient leaves accumulate hydrogen peroxide (H_2O_2) at earlier stages of *Zymoseptoria tritici* infection. **A**, Representative leaf segments from no virus, virus-only control (BSMV:*asGFP*), *phytoene desaturase* (*PDS*)-silenced (BSMV:*asPDS*), and *ChlH*-silenced (BSMV:*asChlH*) wheat cv. Riband, stained for H_2O_2 using diaminobenzidine (DAB) stain at 0, 9, 11, and 14 days postinoculation (dpi) with *Z. tritici*. The darker the brown stain the greater the amount of H_2O_2 present. Also shown are representative leaf segments from healthy (no virus) and virus-treated cv. Riband plants that were cotton wool swab-inoculated with a solution of sterile water supplemented with 0.1% (vol/vol) Silwet L-77 (mock inoculation) and stained for H_2O_2 using DAB. **B**, H_2O_2 levels in control and chlorophyll-deficient mock-inoculated leaves were assayed at 0 dpi using a colorimetric assay. Data shown are mean H_2O_2 levels from six samples from two independent experiments. Error bars represent mean \pm standard error of the mean. The asterisk denotes $P < 0.05$ from an analysis of variance.

and that chloroplast functionality can dictate the frequency of these events in a niche of the host rarely occupied by *Z. tritici*.

DISCUSSION

Plant cell death is a tightly regulated process that is often used to resist certain types of microbial pathogens, the so called biotrophs, that feed on living plant tissue. Conversely, there are many examples of hemibiotrophic and necrotrophic pathogens that appear to activate or exploit the plant cell death response in order to obtain nutrients from the dying tissues (Faris et al. 2010; Dickman and de Figueiredo 2013; Govrin and Levine 2000; Lorang et al. 2012; Oliver and Solomon 2010; Qutob et al. 2006). There are also particular cases in which plant cell

death may play a different role in the outcome of a disease interaction, depending upon its strength and temporal activation. For example, the hemibiotrophic rice blast fungus *Magnaporthe oryzae* and the oomycete *Phytophthora infestans* ultimately kill plant host cells during the course of successful colonization. However, avirulent strains of these pathogens often elicit a more rapid host PCD representative of an HR in particular resistant host plant genotypes, which prevents further colonization and blocks reproductive development (Bryan et al. 2000; Jia et al. 2000; Vleeshouwers et al. 2000). This example serves to emphasize the importance of the correct temporal regulation of plant PCD responses during interactions of plants with hemibiotrophic and necrotrophic pathogens. In this study, we show that the execution of plant PCD during pathogen

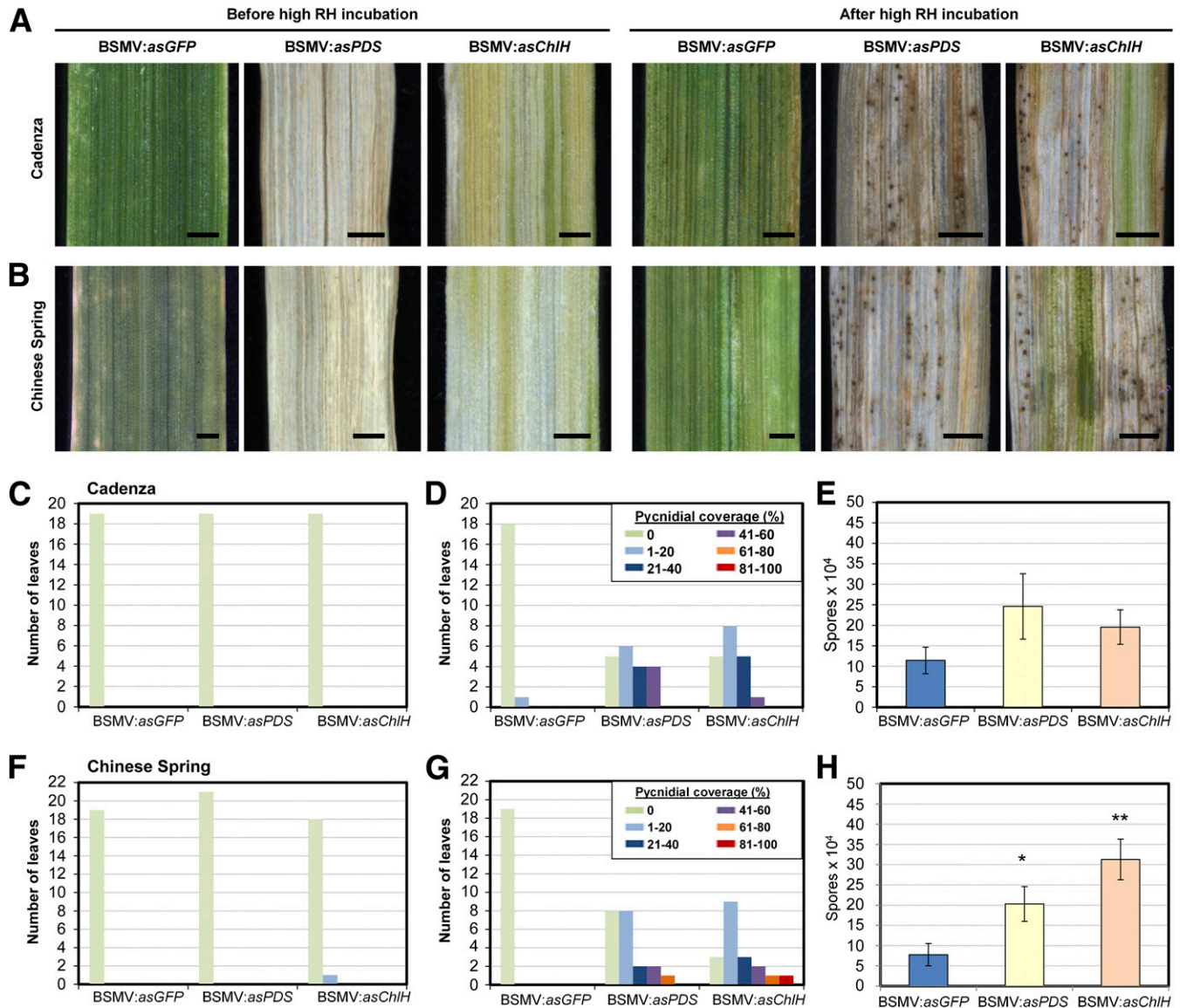


Fig. 6. *Stb6*-mediated resistance to *Zymoseptoria tritici* is partially compromised in chlorophyll-deficient leaf tissue. Virus control-treated (BSMV:asGFP) and chlorophyll-deficient (BSMV:asPDS and BSMV:asChIH) leaves of *Stb6*-carrying wheat cvs. Cadenza and Chinese Spring were inoculated with *Z. tritici*. **A** and **B**, Leaves at 21 days postinoculation (dpi) with *Z. tritici* before and after 48 h of incubation at high relative humidity (RH). Black scale bars represent 1 cm. **C** and **D**, Pycnidial coverage scores on cv. Cadenza leaves at 21 dpi either before further incubation at high relative humidity (**C**) or after 48 h of incubation at high relative humidity (**D**). **E**, Mean pycnidiospores counts in spore washes from detached cv. Cadenza leaves after 48 h of incubation at high RH. **F** and **G**, Pycnidial coverage scores on cv. Chinese Spring leaves at 21 dpi either before (**F**) or after (**G**) 48 h of incubation at high RH. **H**, Mean pycnidiospores counts in spore washes from detached cv. Chinese Spring leaves. Data plotted in **C**, **D**, **F** and **G** are the total number of leaves within each of the six pycnidial coverage score classes, where a total of 19 to 21 leaves per virus treatment were scored over three independent experiments. Data shown in **E** and **H** are mean spore counts from six samples from two independent experiments, each sample comprising 3 × 6-cm-long leaf segments, each leaf from an individual plant. Error bars represent mean ± standard error of the means. Single asterisks denote $P < 0.05$ and double asterisks $P < 0.01$ from restricted maximum likelihood analysis.

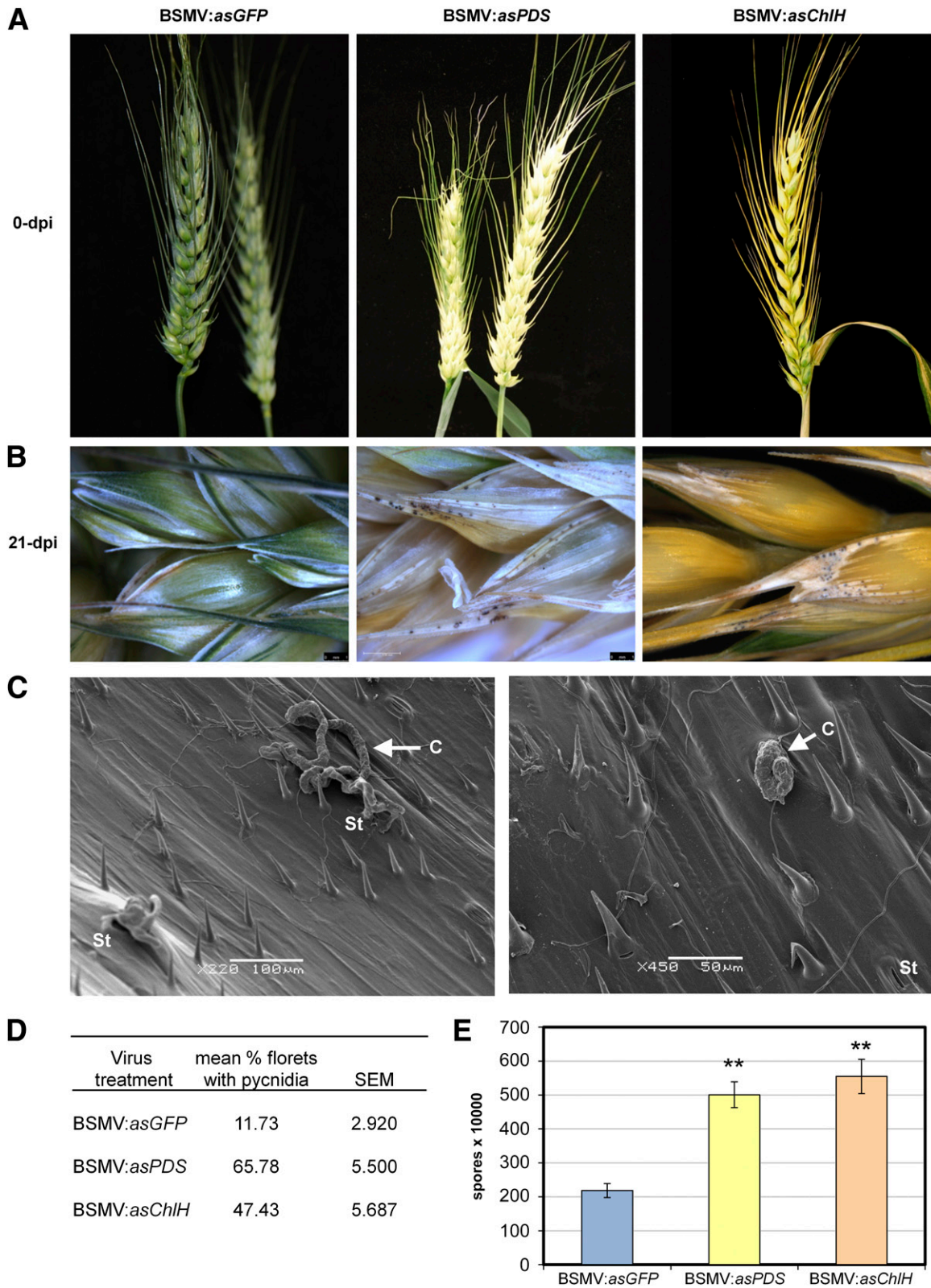


Fig. 7. Increased *Zymoseptoria tritici* infection and effective asexual sporulation on chlorophyll-deficient wheat ears. **A**, The appearance of wheat ears of control (BSMV:asGFP) and chlorophyll-deficient (BSMV:asPDS and BSMV:asChlH) wheat cv. Bobwhite prior to spray-inoculation with *Z. tritici* (0 dpi). **B**, Florets at 21 days postinoculation (dpi) with *Z. tritici*. Images are representative of typical symptoms on the florets of inoculated ears. The clusters of small black dots at the ends of the glumes and on the base of the awns are the pycnidia produced by *Z. tritici*. **C**, Two scanning electron microscope images of the surface of *Z. tritici*-infected glume tissue from *phytoene desaturase* (*PDS*)-silenced (BSMV:asPDS-infected) wheat ears. Cirri (c) can be seen oozing out of stomata onto the glume surface. St, stoma. **D**, A larger percentage of florets on chlorophyll-deficient ears than on control ears develop pycnidia by 21 dpi ($n = 6$; data pooled from two independent experiments). **E**, Mean pycnidiospore counts in spore washes from individual wheat ears. Around 5×10^6 spores were obtained in washes from individual *PDS*-silenced or *Mg-chelatase H subunit* (*ChlH*)-silenced wheat ears, compared with 2×10^6 spores in washes from individual control-treated ears. Data shown are mean spore counts from a minimum of two independent experiments, three samples per experiment. Error bars represent mean \pm standard error of the means. Double asterisks denote $P < 0.01$ from restricted maximum likelihood analysis.

colonization is influenced by chloroplast functionality and regulates the levels of pathogen reproduction in differing genotype (susceptible and resistant) and tissue (leaves and ears) interactions.

Z. tritici is a major fungal pathogen of wheat leaves under cool and wet conditions. Previous studies have identified changes in chloroplast ultrastructure during particular phases of a fully susceptible interaction between wheat and *Z. tritici* (Kema et al. 1996). Other studies have identified at least two phases to the compatible interaction, an initial symptomless phase in which the fungus grows at low density in the absence of host tissue death, followed by a rapid transition to leaf-lesion formation, which is accompanied by rapid plant cell death and rapid increases in *Z. tritici* hyphal biomass presumed to be due to the fungus feeding as a necrotroph (Kema et al., 1996; Keon et al. 2007; Rudd et al. 2008; Shetty et al. 2003). Shading of infected leaves has been shown to retard the development of chlorosis and necrotic cell death during the transition to fungal necrotrophic growth (Keon et al. 2007). Collectively, these earlier studies suggest roles for chloroplasts in influencing disease interactions with *Z. tritici* in wheat leaves. In this study, we investigated the effect of silencing two genes that have key roles in photosynthetic pigment biosynthesis and, thereby, in chloroplast function, on *Z. tritici*-induced cell death, disease symptom development, and spore production (asexual reproduction).

The one or more mechanisms by which *Z. tritici* induces host PCD during leaf lesion formation, which is the hallmark for the rapid transition to necrotrophic feeding by *Z. tritici*, are as yet unknown. This process exhibits markers of apoptosis (Keon et al. 2007; Rudd et al. 2008). *PDS*- and *ChlH*-silenced leaves of the *Z. tritici*-susceptible wheat cv. Riband displayed accelerated cell death in response to *Z. tritici* infection (Fig. 4). Genomic DNA laddering, one of the hallmarks of PCD, was detected in 7- and 9-dpi samples from *Z. tritici*-infected *PDS*-silenced leaves, suggesting that the cell death observed was PCD rather than uncontrolled cellular disintegration. Although the integrity of genomic DNA in *ChlH*-silenced leaf tissue was not assayed over the course of *Z. tritici* infection, it seems likely that PCD is also involved in the cell-death response of these leaves to fungal infection. Despite triggering accelerated cell death, *Z. tritici* appeared to be unable to form pycnidia in chlorophyll-deficient leaves, unless the leaves were subsequently incubated at high RH conditions. Furthermore, the pycnidia that did form at high RH released fewer asexual spores (pycnidiospores), suggesting that *PDS*- and *ChlH*-silenced leaves are less able to support asexual sporulation of *Z. tritici*. These data also indicate that the processes involved in *Z. tritici* pycnidial structure formation and in spore formation and maturation can be uncoupled, as is the case with the related dothideomycete wheat leaf necrotroph *Stagonospora nodorum* (Du Fall and Solomon 2013). The acceleration of host PCD during *Z. tritici* infection on chlorophyll-deficient leaves effectively resulted in early transition from the symptomless phase to the necrotrophic phase of the fungal infection cycle. Our data, therefore, suggest that premature or deregulated host PCD during *Z. tritici* infection can affect the ability of the fungus to subsequently complete its asexual lifecycle on wheat leaves.

The inability of *Z. tritici* to form pycnidia and sporulate on chlorophyll-deficient leaves could be due to insufficient availability of nutrients in the nonphotosynthetic *PDS*- and *ChlH*-silenced leaf tissues, which presumably function as carbon sinks during plant development. However, the fungus was subsequently able to form pycnidial structures after incubation at high RH, even when the chlorophyll-deficient leaves were detached from the rest of the wheat plants (Fig. 1) and cannot,

therefore, be importing nutrients from other plant tissues. This indicates there are sufficient resources in chlorophyll-deficient leaf tissue to support pycnidial formation and permit limited sporulation once an increase in RH occurs. However, it is possible that some of these nutritional resources are not accessible to the fungal hyphae in the prematurely dying chlorophyll-deficient leaf tissue until the leaves are incubated at high RH. Partial rehydration may, perhaps, lead to the release of any remaining cellular contents.

Interfering with the carotenoid and chlorophyll biosynthesis pathways affects the accumulation of a number of key plant hormones and signaling compounds. The biosynthetic pathways of three key plant defense signaling molecules, SA, JA, and NO, each involve steps within the chloroplast (Creelman and Mullet 1997; Ishiguro et al. 2001; Jasid et al. 2006; Strawn et al. 2007). In addition, the carotenoid biosynthesis pathway interacts with those for abscisic acid (ABA) and gibberellic acid biosynthesis, among others, while ChlH, itself, is an ABA receptor (Shen et al. 2006). It is possible that *Z. tritici* infection may trigger a further imbalance of various key signaling molecules in *PDS*- and *ChlH*-silenced leaves, which could result in the premature activation of host PCD. We originally selected these two wheat genes for analysis in combination with *Z. tritici* infection assays because both have the added advantage of generating clear phenotypes (photobleaching or yellowing) when efficient silencing has been triggered via transient BSMV-mediated VIGS.

Disease lesion formation and asexual reproduction in susceptible plants has been shown to be associated with high levels of ROS appearing in *Z. tritici*-infected wheat leaves (Keon et al. 2007; Shetty et al. 2003). In this study, we demonstrate that *PDS*- and *ChlH*-silenced leaves show more rapid accumulation of H₂O₂ during *Z. tritici* infection as well as elevated ROS levels prior to inoculation, in the case of *ChlH*-silenced leaves. It was not possible to ascertain the subcellular origin of these ROS, although it was clear that H₂O₂ accumulated in the mesophyll and not in the epidermal cell layer. There was no evidence of the generation of ROS by the *Z. tritici* hyphae. The abundance of H₂O₂ suggests that the premature activation of host PCD may coincide with earlier activation of ROS signaling. That ROS play important roles in defense signaling and the activation of PCD is generally well accepted, although the differential roles and contributions of different ROS species originating from the various subcompartments of the cell are still not clearly understood (Galvez-Valdivieso and Mullineaux 2010; Kangasjärvi et al. 2012; Sierla et al. 2013). However, at this stage, we cannot conclude that ROS-related changes underpin each of the phenotypic alterations observed in this study. For example, other studies have shown that chloroplasts develop abnormally in plants in which *PDS* or genes that encode Mg chelatase subunits have been silenced (Wang et al. 2009; Luo et al. 2013). Chloroplasts in yellow *ChlD*- and *ChlI*-silenced pea leaf tissue lacked complete stromal thylakoid membranes and grana stacks (Luo et al. 2013), whereas only etioplasts were visible in the white photobleached regions of *PDS*-silenced transgenic tobacco (*Nicotiana tabacum*) leaves (Wang et al. 2009).

Although we did not investigate the ultrastructure of the chloroplasts in *PDS*- and *ChlH*-silenced wheat leaves in this study, it is highly likely that chloroplastic development or morphology was affected by the silencing of these key two enzymes required for photopigment biosynthesis. In the light microscopy images of the control BSMV:*asGFP*-infected wheat leaves, numerous chloroplasts were clearly visible in each of the mesophyll cells in the leaf tissue. By contrast, no chloroplast-like structures were visible under the light microscope in the mesophyll cells of either *PDS*- or *ChlH*-silenced

leaves, perhaps indicating that the chloroplasts were either under-developed or did not develop from etioplasts at all, as was the case in *PDS*-silenced tobacco plants (Wang et al. 2009).

Potentially, the developing chloroplasts in *PDS*- and *ChlH*-silenced wheat leaves are more prone to damage when other key stress-related signaling pathways are induced in response to *Z. tritici* infection, and the general leakage of ROS and other metabolites from the chloroplast might then contribute toward activation of host cell death. In this context, it is worth reiterating that chloroplast ultrastructural abnormalities are one of the earliest subcellular responses of wheat leaves during infection by compatible isolates of *Z. tritici* (Kema et al. 1996).

Curiously, by 21 dpi, *Z. tritici* hyphae were less visible in the collapsed tissue in *PDS*-silenced susceptible wheat leaves (cv. Riband) but, instead, appeared to be under the leaf cuticle. It is possible that the fungal hyphae had grown preferentially toward the subcuticular space for protection against desiccation in the dead and drying tissue of *PDS*-silenced leaves, as leaf desiccation is the eventual outcome of *Z. tritici*-induced PCD. However, a change in the spatial distribution of the *Z. tritici* mycelium did not occur in *ChlH*-silenced leaves, in which fungal hyphae were still visible around the collapsed mesophyll cells. We speculated that *Z. tritici*-induced host PCD might have been more rapid in *PDS*-silenced leaves than in *ChlH*-silenced tissue, perhaps due to the residual presence of protective carotenoids in *ChlH*-silenced but not in *PDS*-silenced leaves, resulting in the *PDS*-silenced *Z. tritici*-infected leaves becoming desiccated more rapidly than *ChlH*-silenced leaves. Interestingly, in several other compatible fungal-plant interactions, for example the *Rhynchosporium commune*-barley interaction, fungal hyphae are known to naturally preferentially accumulate below the leaf cuticle (Lyngs Jørgensen et al. 1993).

Asexual sporulation of *Z. tritici* was, therefore, significantly reduced on *PDS*- and *ChlH*-silenced leaves of susceptible wheat plants, probably as a consequence of the more rapid tissue death. By contrast, and somewhat unexpectedly, pycnidia formation was enhanced on chlorophyll-deficient leaves of wheat cultivars possessing the *Stb6* resistance gene required for gene-for-gene resistance against *Z. tritici* IPO323. Thus, the one or more mechanisms underpinning *Stb6*-mediated resistance had been compromised, at least in part, by the alterations to chloroplast function. As *Stb6*-directed resistance occurs in the absence of host PCD (Kema et al. 1996; Rudd et al. 2008), one possibility is that loss of chloroplast functionality makes resistant leaves more liable to undergo cell death, which *Z. tritici* is able to utilize to support some degree of asexual reproduction. It should be noted that only relatively small numbers of pycnidiospores were present in washes from the chlorophyll-deficient leaves of these cultivars relative to the amounts collected from leaves of fully susceptible cultivars. Approximately between 2×10^5 to 3×10^5 spores were recovered from 3 × 6-cm-long sections of chlorophyll-deficient leaves of *Z. tritici*-inoculated resistant cvs. Chinese Spring and Cadenza (Fig. 6E and H). By contrast, 9×10^6 spores were present in washes from leaf sections of an equivalent size taken from control-treated susceptible wheat cv. Riband (Fig. 2C). Nevertheless, there were clearly significantly more spores washed from chlorophyll-deficient leaf segments of cv. Chinese Spring than from the corresponding virus control-treated leaf segments ($P < 0.05$, LSD). Interestingly, although markedly more *Z. tritici* spores were washed from chlorophyll-deficient than from control-treated leaves of cv. Cadenza, this increase in spore numbers was not statistically significant (Fig. 6E). In this work, we have not attempted to identify mechanisms for this phenotypic difference observed between the two resistant cultivars tested. However, it was noted that silencing *ChlH* led

to accumulation of higher basal levels of H_2O_2 in cv. Chinese Spring but not in cv. Cadenza, so it could be speculated that there might be a difference in the ability of the two cultivars to regulate ROS production, either in general or only when chloroplast function is greatly affected. A recent study in which the Mg chelatase subunits *ChlD* and *ChlI* were silenced in pea (*Pisum sativum*) leaves demonstrated that leaves with reduced activity of these enzymes accumulated higher levels of both H_2O_2 and O_2^- than green leaves and that this increased ROS accumulation was more pronounced if light illumination intensity was increased (Luo et al. 2013). It appears, therefore, that alterations in Mg chelatase activity disrupt the balance between ROS production and ROS detoxification (Luo et al. 2013), and it may be that the ability to maintain ROS homeostasis when chloroplast function is compromised differs between different wheat genotypes. However, DNA polymorphism analysis at the whole-genome level has revealed that the two resistant spring cultivars used in this current study were quite dissimilar (Allen et al. 2013). Therefore, differences at other genetic loci may be responsible for the more pronounced effect on *Z. tritici* sporulation observed in cv. Chinese Spring compared with that seen in cv. Cadenza.

In several other cereal pathosystems investigated using BSMV-mediated VIGS, fungal pathogens have been inoculated onto *PDS*-silenced leaves in which photobleaching was used predominantly as a visual marker for successful VIGS. To date, silencing of *PDS* has been reported to have no effect on *Mla13*-mediated resistance to powdery mildew (*Blumeria graminis* f. sp. *hordei*) in barley (Hein et al. 2005). Similarly, silencing *PDS* did not appear to affect either the compatible or incompatible interaction of wheat cultivars with an isolate of the leaf rust pathogen *Puccinia triticina* (Scofield et al. 2005). The differential effect observed here in the *Z. tritici*-wheat interaction is presumably due to the difference in pathogenic lifestyle between the various fungal species. *B. graminis* f. sp. *hordei* and *P. triticina* are both obligate biotrophic pathogens that form intracellular feeding structures called haustoria. On the other hand, *Z. tritici* infection on wheat is exclusively extracellular and involves a late necrotrophic stage accompanied by the induction of some form of active host PCD (Keon et al. 2007).

Repka (2002) described a chlorophyll-deficient mutant of oak (*Quercus petraea* L.) that showed constitutive accumulation of H_2O_2 and an accelerated HR-like cell death response to the powdery mildew *Erysiphe cichoracearum*, resulting in enhanced resistance to this fungal disease. However, it should be noted that sporadic cell death was observed in leaves of this oak mutant, which was not apparent in *PDS*- or *ChlH*-silenced wheat leaves in the absence of fungal inoculation. This could explain why enhanced resistance to a biotrophic pathogen was observed in this oak mutant but not reported to occur in the *PDS*-silenced barley following inoculation with adapted powdery mildew species (Hein et al. 2005).

Significantly, in this study, silencing of *PDS* or *ChlH* rendered wheat ears more susceptible to *Z. tritici* infection, resulting in greater levels of *Z. tritici* asexual sporulation on the glumes. This is important because *Z. tritici* is regarded as predominantly a foliar pathogen and has been reported only rarely in wheat ears in the field. Nonetheless, at high inoculum pressure, *Z. tritici* developed pycnidia even on nonsilenced wheat ears. Pycnidia formation on green ears sprayed with very high *Z. tritici* concentrations (1×10^7 spores per milliliter) was only observed in the green (chlorophyll-containing) regions of the glume and awn tissues, indicating that the chloroplast plays an important role in dictating the ability of *Z. tritici* to infect and reproduce in ear tissues. Similarly, in *PDS*- and *ChlH*-silenced ears, pycnidia only developed on the equivalent

regions of the photobleached glumes and awns, in which the chloroplasts reside, but a lower concentration of *Z. tritici* inoculum was required to achieve a high infection rate on the individual florets of photobleached ears (Fig. 7). Our observations imply that fluctuations or reduction in chloroplast functionality in wheat ears, which can occur in the field as a result of high light, nutrient, or other biotic and abiotic stresses, could potentially dictate the frequency of *Z. tritici* asexual sporulation in the wheat ear tissue following infection by either airborne ascospores or rain-splashed pycnidiospores. In our bioassays, around 10 million spores were washed from each leaf sample, with each leaf sample comprising three 6-cm long leaf segments or roughly two-thirds of a whole leaf of the equivalent developmental stage. Importantly, we show that up to approximately 5 million spores can be produced on single chlorophyll-deficient wheat ears under optimal conditions (Fig. 7E). Thus, there is clearly potential for wheat ears to be a substantial source of *Z. tritici* pycnidiospores, particularly in cultivars in which ears remain close to the flag leaves in the canopy and are, therefore, more likely to be exposed to pycnidiospores produced on wheat leaf tissue.

The chloroplast has multiple, interconnected roles in cellular stress signaling, and this study has not attempted to elucidate which defense signaling pathway or pathways are involved in *Z. tritici* interactions within wheat leaves or ears. Instead, we have shown that chloroplast functionality and the role of this organelle on the regulation of host cell death has a strong influence on the outcome of these different *Z. tritici*-wheat interactions and is capable of dictating the incidence of asexual reproduction of this fungal pathogen on wheat tissues through interacting with the plant cell death machinery. In addition, this study highlights the importance of the exact timing of *Z. tritici*-triggered cell death in determining whether or not this exclusively apoplastically dwelling fungal pathogen is able to complete its asexual lifecycle and that chloroplast functionality is an important regulator of this process. This implies that priming normally susceptible plants for earlier (more rapid) cell death during *Z. tritici* infection could be a useful means of reducing or blocking polycyclic crop infections that result from effective asexual reproduction.

MATERIALS AND METHODS

Plant growth conditions.

Nicotiana benthamiana for preparation of BSMV sap inoculum and wheat (*Triticum aestivum*) were raised in Levington F2+S Seed & Modular Compost Plus Sand and Rothamsted prescription mix compost (Petersfield Products), respectively, in a controlled environment room with day and night temperatures of 23 and 20°C, respectively, 60% RH, and a 16-h photoperiod (approximately 180 $\mu\text{mol}\cdot\text{m}^{-2}\cdot\text{s}^{-1}$ light). Seedlings of the wheat cv. Riband, susceptible to *Z. tritici* isolate IPO323, and of cvs. Cadenza and Chinese Spring, carrying the *Stb6* gene for resistance to *Z. tritici* isolate IPO323, were grown in 5-cm-deep trays measuring 22 by 15 cm for the attached leaf infection bioassays. Wheat cv. Bobwhite plants (susceptible to *Z. tritici* isolate IPO323) were grown singly in 8 × 8 × 9 cm square-sided pots for the ear-inoculation bioassays.

BSMV VIGS constructs and virus inoculations.

The BSMV-VIGS system described by Yuan et al. (2011), comprising three T-DNA binary plasmids, pCaBS- α , pCaBS- β , and pCa- γ bLIC, was used. To generate the gene-silencing construct targeting wheat *PDS* (*TaPDS*; GenBank accession FJ517553), a 185-bp fragment of *TaPDS* was amplified, using PCR, from wheat cv. Cadenza leaf cDNA, using the primer pair LIC asTaPDS F (5'-AAGGAAGTTTAAGGGAAATCAAAA

CGGCTGTA-3') and LIC asTaPDS R (5'-AACCACCACCACCGTGTGCATGGAAGGATGAAGA-3'). This fragment was cloned into pCa- γ bLIC in antisense orientation. BSMV: *TaChlH*₂₅₀ generated by Yuan et al. (2011) was used to target wheat *ChlH* (The Institute for Genomic Research accession TC169257), while BSMV:asGFP, described by Lee et al. (2014), was used as a negative control virus treatment.

Transformation of BSMV binary plasmids into *Agrobacterium tumefaciens* GV3101 and agroinfiltration into 3- to 4-week-old *N. benthamiana* plants was carried out as described previously (Lee et al. 2014). Sap from the infiltrated leaves was used to mechanically inoculate either the first leaves of 11-day-old wheat plants, for *Z. tritici* attached-leaf infection assays, or the fourth or fifth leaf of 7-week-old plants, for *Z. tritici* ear infection assays.

Fungal strains, wheat leaf, and ear inoculations and fungal disease assessment.

The *Z. tritici* isolate IPO323 was used in all experiments in this study. The isolate was stored at -80°C in 50% (vol/vol) glycerol. Fungal conidiospores for plant inoculation were harvested from 7-day-old yeast peptone dextrose agar cultures grown at 16°C into sterile water supplemented with 0.1% (vol/vol) Silwet L-77 (GE Silicones). A fungal inoculum was adjusted to 5 × 10⁶ conidiospores per milliliter and was applied to the third leaves of 25-day-old wheat plants. Attached wheat leaf infection assays and disease assessment at 21 dpi were carried out as described previously (Lee et al. 2014).

After visual disease assessment at 21 dpi, 6-cm-long segments of the *Z. tritici*-inoculated wheat leaves were detached and were then placed in sterile 15-ml tubes (Greiner Bio-one) for high-RH incubations. Three segments, each from an individual wheat leaf, were incubated in each tube. The tubes were plugged with cotton wool saturated with sterile water before the lids were replaced, and the tubes were incubated without opening at 15°C for 48 h in the dark. Following high-RH incubation, the leaf segments were assessed for disease by scoring the area of *Z. tritici*-inoculated leaf tissue that was both necrotic and evenly covered by fungal pycnidia. The scores were sorted into six pycnidial coverage classes: 0, 1 to 20, 21 to 40, 41 to 60, 61 to 80, and 80 to 100%. All disease assessments were made by the same person.

After the leaf segments had been assessed for pycnidial coverage, 2 ml of sterile water was added to each tube containing three leaf segments. The combined area of the three leaf segments corresponded to approximately one half to two thirds of one whole wheat leaf of a similar age and developmental stage. The tubes were vortexed vigorously for 30 s to wash pycnidiospores off before the leaf segments were discarded, and spores were counted, using a hemocytometer (Hausser Scientific) with the aid of a light microscope. Pycnidiospores from a minimum of three replicate samples from each virus treatment were counted in each experiment.

Ears of wheat in the preanthesis stage were spray-inoculated with *Z. tritici* conidiospores at a concentration of 5 × 10⁶ spores per milliliter in sterile water containing 0.1% (vol/vol) Silwet L-77 (GE Silicones), and the plants were incubated at high RH (>90%) for 72 h before returning to standard RH (approximately 60%) for up to 20 days. Fungal disease on inoculated wheat ears was assessed at 21 dpi by determining the number of (fertile) florets on which *Z. tritici* pycnidia could be observed as a percent of the total number of (fertile) florets on the ear. Individual ears were then removed and were placed individually in 50-ml tubes (Greiner Bio-one). The tubes were plugged with cotton wool saturated with sterile water, were lidded, and were then incubated at high RH without opening at 15°C for 72 h in the dark. Spores were washed from

individual ears by vigorous vortexing for 30 s after adding 2 ml of sterile water. The ears were then removed and replaced inside the tube upside down, and the tubes were vortexed for another 30 s before the ears were discarded and the spores were counted, using a hemocytometer and a light microscope.

Cryo-SEM.

Sections of wheat leaves (about 5 × 5 mm) or entire glumes of *Z. tritici*-inoculated ears were excised using a sterile blade and forceps. The samples were attached to cryo stubs using a smear of OCT compound (Agar Scientific), slotted stubs were used for the freeze-fracturing of leaf tissue. Mounted samples were plunged into liquid nitrogen and were then transferred under vacuum to the Alto 2100 cryo chamber (Gatan), with the stage temperature maintained at -180°C. Leaf sections were fractured using the cold blade mounted in the chamber, followed by sublimation to remove any ice on the surfaces. This was done by raising the temperature of the stage to -95°C for 1 min. Once the temperature recovered to -150°C the samples were coated with gold for 1 min (approximately 10 nm thickness). Glume tissue samples were sublimed to remove ice and were then coated without fracturing. All samples were transferred to the JSM LVSEM 6360 scanning electron microscope (Jeol, Ltd.), with the stage temperature maintained at -150°C for examination and imaging. Operation conditions were 5 kV, high vacuum mode and images were saved using the on-board software (Jeol Ltd.).

Ion-leakage assays.

All assays were conducted in duplicate, with each sample containing two leaf segments of approximately 3 cm. Each leaf segment was taken either from individual *Z. tritici*-inoculated or mock fungus-inoculated leaves. The leaf segments were added to 5 ml of deionized water (bathing solution) and were incubated for 90 min at room temperature. Postincubation, the leaves were removed, the bathing solution was vortexed, and the ionic strength was monitored using a conductivity meter (Model 3540; Jenway).

Genomic DNA extraction and gel electrophoresis.

Genomic DNA was isolated from approximately 60 mg of infected leaf tissue (two 3-cm leaf segments) harvested at 0, 7, 9, and 13 days post-*Z. tritici* inoculation, using a DNeasy plant mini kit (Qiagen), following the supplier's instructions. DNA integrity was analyzed by electrophoresis on a 0.8% agarose gel.

Trypan blue staining for fungal hyphae and dead plant cells.

Leaf sections of 3 cm in length were removed at various time points postinoculation with *Z. tritici* and were stained with lactophenol trypan blue (Keogh et al. 1980). Samples were immersed in trypan blue stain and were then boiled in a 95°C water bath for 3 min, before being allowed to cool to room temperature. Samples were left in trypan blue overnight, at room temperature, before being transferred to chloral hydrate solution (250 g per 100 ml of water) on a Zeiss Axiophot microscope (Carl Zeiss Microscopy Ltd.) using bright-field illumination.

DAB staining for H₂O₂.

Wheat leaves were collected immediately prior to *Z. tritici* inoculation (0 dpi samples) or at 9, 11, and 14 days post-*Z. tritici* inoculation. The leaves were cut into 3-cm segments and were then incubated overnight in the presence of DAB (Sigma) at 1 mg/ml, dissolved in water (pH 3.8), in the dark in order to stain for H₂O₂, as described by Thordal-Christensen et al. (1997). The stained leaf material was cleared by incubating

overnight in 3:1 ethanol/acetic acid solution (vol/vol) in 15-ml tubes with rotation of 30 rpm on a Stuart SRT6D roller mixer. The cleared leaves were rinsed and stored in a petri dish on paper towels saturated with a lactoglycerol solution (lactic acid/glycerol/water in 1:1:1 [vol/vol/vol] ratios), as described by Liu et al. (2012).

Hydroxide peroxide measurements.

Total H₂O₂ per gram of leaf tissue was determined according to the method described by Ding et al. (2009), with minor modifications. Wheat leaf samples of 0.15 g were ground to a fine powder in liquid nitrogen. Each sample contained approximately three 5-cm-long segments, each segment from an individual wheat leaf. The powder was extracted in 1 M HClO₄ and 5% insoluble polyvinylpyrrolidone. The homogenate was centrifuged at 12,000 × *g* for 10 min, and the supernatant was neutralized with 5 M K₂CO₃ in the presence of 50 μl of 0.3 M phosphate buffer (pH 5.6). Samples were centrifuged at 12,000 × *g* for 1 min to remove KClO₄, and the supernatant was incubated for 10 min with 1 U ascorbate oxidase (Sigma) at room temperature. The reaction mixture, comprising 0.1 M phosphate buffer (pH 6.5), 3.3 mM 3-(dimethylamino) benzoic acid, and 0.07 mM 3-methyl-2-benzothiazoline hydrazone, was prepared in individual cuvettes. Just prior to reaction initiation, 0.1 U horseradish peroxidase (Sigma) was added to the reaction mixture. The reaction was initiated by the addition of 50 μl of sample, and the absorbance change at 590 nm was monitored at 25°C for 4 min. In order to quantify the H₂O₂ content in the samples by reference to an internal standard, 2 nmol H₂O₂ was added to a second aliquot of sample and was assayed in parallel to the first aliquot of each sample.

Statistical analyses.

GenStat (release 16.1, 2013, VSN International Ltd.) was used for the statistical analyses. Percent pycnidial coverage of wheat leaves from *Z. tritici* inoculation experiments were analyzed using generalized linear modeling assuming a Poisson distribution with a natural logarithm link function. The variate modeled was the number of leaves within each pycnidial coverage class for each BSMV-VIGS construct treatment group, accounting for replicate experiments as a blocking term in the model. The condition factors of pre- and posthigh RH incubation were nested within the disease category (pycnidial coverage class). Percent pycnidial coverage for leaves of wheat cv. Riband was analyzed separately from those for the cvs. Chinese Spring and Cadenza leaves. Significance of model terms was assessed using approximate *F* tests. Calculated mean counts were output with standard errors for the statistically significant (*P* < 0.05, *F* test) terms that needed to be considered. Analysis of percent pycnidial coverage on leaves of cvs. Chinese Spring and Cadenza indicated that there was no significant difference between the two cultivars (*P* = 0.714, *F* test) and, therefore, only the calculated means disregarding cultivar effect from this analysis are presented. Biologically important comparisons of calculated means were made using approximate LSD values at the 5% (*P* < 0.05) level of significance.

Differences in H₂O₂ levels assayed colorimetrically in control-treated and chlorophyll-deficient (*PDS*- or *ChlH*-silenced) mock-inoculated leaves of cv. Riband were analyzed using one-way analysis of variance (ANOVA), accounting for the two experiments as blocking terms in the model. Calculated mean values and standard errors of differences of means were output and are displayed in Supplementary Table S3. Significance of difference between mean H₂O₂ values was determined using LSD at the 5% level of significance.

Spore wash count data from control-treated and chlorophyll-deficient *Z. tritici*-inoculated wheat leaves or ears were

analyzed using REML (restricted maximum likelihood) linear mixed modeling fitted to log-transformed spore count values. Significance of difference between mean spore counts was determined using LSD at the 5% and 1% ($P < 0.01$) levels of significance. Calculated means and LSD values are displayed in Supplementary Tables S4 to S11. Pycnidia coverage data from *Z. tritici*-inoculated wheat cv. Bobwhite ears were analyzed using REML linear mixed modeling. The variate modeled was the percent of florets that developed *Z. tritici* pycnidia on virus control-treated and *PDS*- and *ChlH*-silenced ears by 21 dpi. Significance of difference between mean percent of florets that developed pycnidia were made using approximate LSD values at the 5% and 1% levels of significance (Supplementary Table S12).

ACKNOWLEDGMENTS

We thank S. Powers (Rothamsted Research) for help with statistical analyses, G. Shephard (Rothamsted Visual Communications Unit) for assistance with photography of DAB-stained leaves, and K. Halsey for advice on light microscopy techniques. D. Li (China Agricultural University) kindly provided binary BSMV clones and the BSMV:TaChlH₂₅₀ control construct. The work was supported by the Biotechnology and Biological Sciences Research Council of the U.K. (BBSRC) through the Institute Strategic Programme Grant 20:20 Wheat (BB/J00426X/1). This research was carried out under the Fera agency of the U.K. Department for Environment, Food and Rural Affairs plant health license PHSI 181/6786.

LITERATURE CITED

Allen, A. M., Barker, G. L. A., Wilkinson, P., BurrIDGE, A., Winfield, M., Coghill, J., Uauy, C., Griffiths, S., Jack, P., Berry, S., Werner, P., Melichar, J. P., McDougall, J., Gwilliam, R., Robinson, P., and Edwards, K. J. 2013. Discovery and development of exome-based, co-dominant single nucleotide polymorphism markers in hexaploid wheat (*Triticum aestivum* L.). *Plant Biotechnol. J.* 11:279-295.

Asada, K. 1999. The water-water cycle in chloroplasts: Scavenging of active oxygens and dissipation of excess photos. *Annu. Rev. Plant Physiol. Plant Mol. Biol.* 50:601-639.

Asselbergh, B., Curvers, K., Franca, S. C., Audenaert, K., Vuylsteke, M., Van Breusegem, F., and Höfte, M. 2007. Resistance to *Botrytis cinerea* in *sitiens*, an abscisic acid-deficient tomato mutant, involves timely production of hydrogen peroxide and cell wall modifications in the epidermis. *Plant Physiol.* 144:1863-1877.

Brading, P. A., Verstappen, E. C. P., Kema, G. H. J., and Brown, J. K. M. 2002. A gene-for-gene relationship between wheat and *Mycosphaerella graminicola*, the Septoria tritici blotch pathogen. *Phytopathology* 92: 439-445.

Bryan, G. T., Wu, K. S., Farrall, L., Jia, Y., Hershey, H. P., McAdams, S. A., Faulk, K. N., Donaldson, G. K., Tarchini, R., and Valent, B. 2000. A single amino acid difference distinguishes resistant and susceptible alleles of the rice blast resistance gene *Pi-ta*. *Plant Cell* 12:2033-2046.

Chartrain, L., Brading, P. A., and Brown, J. K. M. 2005. Presence of the *Stb6* gene for resistance to septoria tritici blotch (*Mycosphaerella graminicola*) in cultivars used in wheat-breeding programmes worldwide. *Plant Pathol.* 54:134-143.

Coego, A., Ramirez, V., Gil, M. J., Flors, V., Mauch-Mani, B., and Vera, P. 2005. An *Arabidopsis* homeodomain transcription factor, OVEREXPRESSION OF CATIONIC PEROXIDASE 3, mediates resistance to infection by necrotrophic pathogens. *Plant Cell* 17:2123-2137.

Consolo, V. F., Albani, C. M., Berón, C. M., Salerno, G. L., and Cordo, C. A. 2009. A conventional PCR technique to detect *Septoria tritici* in wheat seeds. *Australas. Plant Pathol.* 38:222-227.

Creelman, R. A., and Mullet, J. E. 1997. Biosynthesis and action of jasmonates in plants. *Annu. Rev. Plant Physiol. Plant Mol. Biol.* 48:355-381.

Dean, R., Van Kan, J. A. L., Pretorius, Z. A., Hammond-Kosack, K. E., Di Pietro, A., Spanu, P. D., Rudd, J. J., Dickman, M., Kahmann, R., Ellis, J., and Foster, G. D. 2012. The top 10 fungal pathogens in molecular plant pathology. *Mol. Plant Pathol.* 13:414-430.

Dickman, M. B., and de Figueiredo, P. 2013. Death be not proud—cell death control in plant fungal interactions. *PLoS Pathog.* 9:e1003542. Published online.

Ding, S., Lu, Q., Zhang, Y., Yang, Z., Wen, X., Zhang, L., and Lu, C. 2009. Enhanced sensitivity to oxidative stress in transgenic tobacco plants with

decreased glutathione reductase activity leads to a decrease in ascorbate pool and ascorbate redox state. *Plant Mol. Biol.* 69:577-592.

Du Fall, L. A. D., and Solomon, P. S. 2013. The necrotrophic effector SnToxA induces the synthesis of a novel phytoalexin in wheat. *New Phytol.* 200:185-200.

Eyal, Z. 1999. The *Septoria tritici* and *Stagonospora nodorum* blotch diseases of wheat. *Eur. J. Plant Pathol.* 105:629-641.

Faris, J. D., Zhang, Z., Lu, H., Lu, S., Reddy, L., Cloutier, S., Fellers, J. P., Meinhardt, S. W., Rasmussen, J. B., Xu, S. S., Oliver, R. P., Simons, K. J., and Friesen, T. L. 2010. A unique wheat disease resistance-like gene governs effector-triggered susceptibility to necrotrophic pathogens. *Proc. Natl. Acad. Sci. USA* 107:13544-13549.

Galvez-Valdivieso, G., and Mullineaux, P. M. 2010. The role of reactive oxygen species in signalling from chloroplasts to the nucleus. *Physiol. Plant.* 138:430-439.

Goodwin, S. B. 2012. Resistance in wheat to septoria diseases caused by *Mycosphaerella graminicola* (*Septoria tritici*) and *Phaeosphaeria* (*Stagonospora nodorum*). Pages 151-159 in *Disease Resistance in Wheat*, 2012, I. Sharma, ed. CABI, Wallingford, U.K.

Goodwin, S. B., M'barek, S. B., Dhillon, B., Wittenberg, A. H. J., Crane, C. F., Hane, J. K., Foster, A. J., Van der Lee, T. A., Grimwood, J., Aerts, A., Antoniw, J., Bailey, A., Bluhm, B., Bowler, J., Bristow, J., van der Burgt, A., Canto-Canché, B., Churchill, A. C., Conde-Ferraz, L., Cools, H. J., Coutinho, P. M., Csukai, M., Dehal, P., De Wit, P., Donzelli, B., van de Geest, H. C., van Ham, R. C., Hammond-Kosack, K. E., Henrissat, B., Kilian, A., Kobayashi, A. K., Koopmann, E., Kourmpetis, Y., Kuzniar, A., Lindquist, E., Lombard, V., Maliepaard, C., Martins, N., Mehra, R., Nap, J. P., Ponomarenko, A., Rudd, J. J., Salamov, A., Schmutz, J., Schouten, H. J., Shapiro, H., Stergiopoulos, I., Torriani, S. F., Tu, H., de Vries, R. P., Waalwijk, C., Ware, S. B., Wiebenga, A., Zwiers, L. H., Oliver, R. P., Grigoriev, I. V., and Kema, G. H. 2011. Finished genome of the fungal wheat pathogen *Mycosphaerella graminicola* reveals dispensable structure, chromosome plasticity, and stealth pathogenesis. *PLoS Genet.* 7:e1002070. Published online.

Govrin, E. M., and Levine, A. 2000. The hypersensitive response facilitates plant infection by the necrotrophic pathogen *Botrytis cinerea*. *Curr. Biol.* 10:751-757.

Hein, I., Barciszewska-Pacak, M., Hrubikova, K., Williamson, S., Dinesen, M., Soenderby, I. E., Sundar, S., Jarmolowski, A., Shirasu, K., and Lacomme, C. 2005. Virus-induced gene silencing-based functional characterization of genes associated with powdery mildew resistance in barley. *Plant Physiol.* 138:2155-2164.

Hiriart, J.-B., Lehto, K., Tyystjärvi, E., Junttila, T., and Aro, E.-M. 2002. Suppression of a key gene involved in chlorophyll biosynthesis by means of virus-inducing gene silencing. *Plant Mol. Biol.* 50:213-224.

Horbach, R., Navarro-Quesada, A. R., Knogge, W., and Deising, H. B. 2011. When and how to kill a plant cell: Infection strategies of plant pathogenic fungi. *J. Plant Physiol.* 168:51-62.

Ishiguro, S., Kawai-Oda, A., Ueda, J., Nishida, I., and Okada, K. 2001. The *DEFECTIVE IN ANther DEHISCENCE* gene encodes a novel phospholipase A1 catalyzing the initial step of jasmonic acid biosynthesis, which synchronizes pollen maturation, anther dehiscence, and flower opening in *Arabidopsis*. *Plant Cell* 13:2191-2209.

Jasid, S., Simontacchi, M., Bartoli, C. G., and Puntarulo, S. 2006. Chloroplasts as a nitric oxide cellular source. Effect of reactive nitrogen species on chloroplastic lipids and proteins. *Plant Physiol.* 142: 1246-1255.

Jia, Y., McAdams, S. A., Bryan, G. T., Hershey, H. P., and Valent, B. 2000. Direct interaction of resistance gene and avirulence gene products confers rice blast resistance. *EMBO J.* 19:4004-4014.

Jing, H. C., Lovell, D., Gutteridge, R., Jenk, D., Kornukhin, D., Mitrofanova, O. P., Kema, G. H., and Hammond-Kosack, K. E. 2008. Phenotypic and genetic analysis of the *Triticum monococcum*-*Mycosphaerella graminicola* interaction. *New Phytol.* 179:1121-1132.

Kangasjärvi, S., Neukermans, J., Li, S., Aro, E.-M., and Noctor, G. 2012. Photosynthesis, photorespiration, and light signalling in defence responses. *J. Exp. Bot.* 63:1619-1636.

Kema, G. H. J., Yu, D. Z., Rijkenberg, F. H. J., Shaw, M. W., and Baayen, R. P. 1996. Histology of the pathogenesis of *Mycosphaerella graminicola* in wheat. *Phytopathology* 86:777-786.

Keogh, R. C., Deverall, B. J., and McLeod, S. 1980. Comparison of histological and physiological responses to *Phakopsora pachyrhizi* in resistant and susceptible soybean. *Trans. Brit. Mycol. Soc.* 74:329-333.

Keon, J., Antoniw, J., Carzaniga, R., Deller, S., Ward, J. L., Baker, J. M., Beale, M. H., Hammond-Kosack, K., and Rudd, J. J. 2007. Transcriptional adaptation of *Mycosphaerella graminicola* to programmed cell death (PCD) of its susceptible wheat host. *Mol. Plant Microbe Interact.* 20:178-193.

- Kumagai, M. H., Donson, J., della-Cioppa, G., Harvey, D., Hanley, K., and Grill, L. K. 1995. Cytoplasmic inhibition of carotenoid biosynthesis with virus-derived RNA. *Proc. Natl. Acad. Sci. USA* 92:1679-1683.
- Lam, E., Kato, N., and Lawton, M. 2001. Programmed cell death, mitochondria and the plant hypersensitive response. *Nature* 411:848-853.
- Lee, W. S., Hammond-Kosack, K. E., and Kanyuka, K. 2012. *Barley stripe mosaic virus*-mediated tools for investigating gene function in cereal plants and their pathogens: Virus-induced gene silencing, host-mediated gene silencing, and virus-mediated overexpression of heterologous protein. *Plant Physiol.* 160:582-590.
- Lee, W.-S., Rudd, J. J., Hammond-Kosack, K. E., and Kanyuka, K. 2014. *Mycosphaerella graminicola* LysM effector-mediated stealth pathogenesis subverts recognition through both CERK1 and CEBiP homologues in wheat. *Mol. Plant Microbe Interact.* 27:236-243.
- Liu, Z., Zhang, Z., Farris, J. D., Oliver, R. P., Syme, R., McDonald, M. C., McDonald, B. A., Solomon, P. S., Lu, S., Shelver, W. L., Xu, S., and Friesen, T. L. 2012. The cysteine rich necrotrophic effector SnTox1 produced by *Stagonospora nodorum* triggers susceptibility of wheat lines harboring *Snn1*. *PLoS Pathog.* 8:e1002467 Published online.
- Lorang, J. M., Sweat, T. A., and Wolpert, T. J. 2007. Plant disease susceptibility conferred by a "resistance" gene. *Proc. Natl. Acad. Sci. USA* 104:14861-14866.
- Lorang, J., Kidarsa, T., Bradford, C. S., Gilbert, B., Curtis, M., Tzeng, S. C., Maier, C. S., and Wolpert, T. J. 2012. Tricking the guard: Exploiting plant defense for disease susceptibility. *Science* 338:659-662.
- Lorrain, S., Vaillieu, F., Balagué, C., and Roby, D. 2003. Lesion mimic mutants: Keys for deciphering cell death and defense pathways in plants? *Trends Plant Sci.* 8:263-271.
- Luo, T., Luo, S., Araújo, W. L., Schlicke, H., Rothbart, M., Yu, J., Fan, T., Fernie, A. R., Grimm, B., and Luo, M. 2013. Virus-induced gene silencing of pea *CHLI* and *CHLD* affects tetrapyrrole biosynthesis, chloroplast development and the primary metabolic network. *Plant Physiol. Biochem.* 65:17-26.
- Lyngs Jørgensen, H. J. L., Deneergaard, E., and Smedegaard-Petersen, V. 1993. Histological examination of the interaction between *Rhynchosporium secalis* and susceptible and resistant cultivars of barley. *Physiol. Mol. Plant Pathol.* 42:345-358.
- Masuda, T. 2008. Recent overview of the Mg branch of the tetrapyrrole biosynthesis leading to chlorophylls. *Photosynth. Res.* 96:121-143.
- Mengiste, T. 2012. Plant immunity to necrotrophs. *Annu. Rev. Phytopathol.* 50:267-294.
- Oliver, R. P., and Solomon, P. S. 2010. New developments in pathogenicity and virulence of necrotrophs. *Curr. Opin. Plant Biol.* 13:415-419.
- Palmer, C.-L., and Skinner, W. 2002. *Mycosphaerella graminicola*: Latent infection, crop devastation and genomics. *Mol. Plant Pathol.* 3:63-70.
- Papenbrock, J., Pfündel, E., Mock, H.-P., and Grimm, B. 2000. Decreased and increased expression of the subunit CHL I diminishes Mg chelatase activity and reduces chlorophyll synthesis in transgenic tobacco plants. *Plant J.* 22:155-164.
- Qin, G., Gu, H., Ma, L., Peng, Y., Deng, X. W., Chen, Z., and Qu, L.-J. 2007. Disruption of *phytoene desaturase* gene results in albino and dwarf phenotypes in *Arabidopsis* by impairing chlorophyll, carotenoid, and gibberellin biosynthesis. *Cell Res.* 17:471-482.
- Qutob, D., Kemmerling, B., Brunner, F., Küfner, I., Engelhardt, S., Gust, A. A., Luberacki, B., Seitz, H. U., Stahl, D., Rauhut, T., Glawischnig, E., Schween, G., Lacombe, B., Watanabe, N., Lam, E., Schlichting, R., Scheel, D., Nau, K., Dodt, G., Hubert, D., Gijzen, M., and Nürnberger, T. 2006. Phytotoxicity and innate immune responses induced by Nep1-like proteins. *Plant Cell* 18:3721-3744.
- Repka, V. 2002. Hydrogen peroxide generated via the octadecanoid pathway is neither necessary nor sufficient for methyl jasmonate-induced hypersensitive cell death in woody plants. *Biol. Plantarum* 45:105-115.
- Rudd, J. J., Keon, J., and Hammond-Kosack, K. E. 2008. The wheat mitogen-activated protein kinases TaMPK3 and TaMPK6 are differentially regulated at multiple levels during compatible disease interactions with *Mycosphaerella graminicola*. *Plant Physiol.* 147:802-815.
- Scotfield, S. R., Huang, L., Brandt, A. S., and Gill, B. S. 2005. Development of a virus-induced gene-silencing system for hexaploid wheat and its use in functional analysis of the *Lr21*-mediated leaf rust resistance pathway. *Plant Physiol.* 138:2165-2173.
- Shen, Y.-Y., Wang, X.-F., Wu, F.-Q., Du, S.-Y., Cao, Z., Shang, Y., Wang, X.-L., Peng, C.-C., Yu, X.-C., Zhu, S.-Y., Fan, R.-C., Xu, Y.-H., and Zhang, D.-P. 2006. The Mg-chelatase H subunit is an abscisic acid receptor. *Nature* 443:823-826.
- Shetty, N. P., Kristensen, B. K., Newman, M. A., Moller, K., Gregersen, P. L., and Jørgensen, H. J. L. 2003. Association of hydrogen peroxide with restriction of *Septoria tritici* in resistant wheat. *Physiol. Mol. Plant Pathol.* 62:333-346.
- Sierla, M., Rahikainen, M., Salojärvi, J., Kangasjärvi, J., and Kangasjärvi, S. 2013. Apoplastic and chloroplastic redox signaling networks in plant stress responses. *Antioxid. Redox Signal.* 18:2220-2239.
- Staal, J., Kaliff, M., Dewaele, E., Persson, M., and Dixelius, C. 2008. *RLM3*, a TIR domain encoding gene involved in broad-range immunity of *Arabidopsis* to necrotrophic fungal pathogens. *Plant J.* 55:188-200.
- Strawn, M. A., Marr, S. K., Inoue, K., Inada, N., Zubieta, C., and Wildermuth, M. C. 2007. *Arabidopsis* isochorismate synthase functional in pathogen-induced salicylate biosynthesis exhibits properties consistent with a role in diverse stress responses. *J. Biol. Chem.* 282:5919-5933.
- Thordal-Christensen, H., Zhang, Z., Wei, Y., and Collinge, D. B. 1997. Subcellular localization of H₂O₂ in plants. H₂O₂ accumulation in papillae and hypersensitive response during the barley-powdery mildew interaction. *Plant J.* 11:1187-1194.
- Triantaphylidès, C., Krischke, M., Hoerberichts, F. A., Ksas, B., Gresser, G., Havaux, M., Van Breusegem, F., and Mueller, M. J. 2008. Singlet oxygen is the major reactive oxygen species involved in photooxidative damage to plants. *Plant Physiol.* 148:960-968.
- Vleeshouwers, V. G., van Dooijeweert, W., Govers, F., Kamoun, S., and Colon, L. T. 2000. The hypersensitive response is associated with host and nonhost resistance to *Phytophthora infestans*. *Planta* 210:853-864.
- Wang, M., Wang, G., Ji, J., and Wang, J. 2009. The effect of *pds* gene silencing on chloroplast pigment composition, thylakoid membrane structure and photosynthesis efficiency in tobacco plants. *Plant Sci.* 177:222-226.
- Williams, B., Kabbage, M., Kim, H. J., Britt, R., and Dickman, M. B. 2011. Tipping the balance: *Sclerotinia sclerotiorum* secreted oxalic acid suppresses host defenses by manipulating the host redox environment. *PLoS Pathog.* 7:e1002107 Published online.
- Wolpert, T. J., Dunkle, L. D., and Ciuffetti, L. M. 2002. Host-selective toxins and avirulence determinants: What's in a name? *Annu. Rev. Phytopathol.* 40:251-285.
- Yuan, C., Li, C., Yan, L., Jackson, A. O., Liu, Z., Han, C., Yu, J., and Li, D. 2011. A high throughput *Barley stripe mosaic virus* vector for virus induced gene silencing in monocots and dicots. *PLoS ONE* 6:e26468 Published online.